2022

An improved wild horse optimization algorithm for reliability based optimal DG planning of radial distribution networks

Mohammed Hamouda Ali

Salah Kamel

Mohamed H. Hassan

See next page for additional authors

Funder: European Union and Enterprise Ireland

Authors

Mohammed Hamouda Ali, Salah Kamel, Mohamed H. Hassan, Marcos Tostado-Véliz, and Hossam Zawbaa

Energy Reports 8 (2022) 582–604

Contents lists available at ScienceDirect

Energy Reports

journal homepage: www.elsevier.com/locate/egyr

Research paper

An improved wild horse optimization algorithm for reliability based optimal DG planning of radial distribution networks

Mohammed Hamouda Ali [a], Salah Kamel [b], Mohamed H. Hassan [b], Marcos Tostado-Véliz [c], Hossam M. Zawbaa [d,e,*]

[a] Department of Electrical Engineering, Faculty of Engineering, AL-Azhar University, Cairo, 11651, Egypt
[b] Department of Electrical Engineering, Faculty of Energy Engineering, Aswan University, Aswan 81528, Egypt
[c] Electrical Engineering Department, University of Jaen, EPS, 23700 Linares, Spain
[d] Faculty of Computers and Artificial Intelligence, Beni-Suef University, Beni-Suef, Egypt
[e] Technological University Dublin, Dublin, Ireland

ARTICLE INFO

Article history:
Received 12 October 2021
Received in revised form 30 November 2021
Accepted 7 December 2021
Available online xxxx

Keywords:
Radial distribution network
Distributed generation
BFS algorithm
Improved wild horse optimization algorithm
Reliability assessment
Monte Carlo Simulation

ABSTRACT

This paper introduces a novel technique for optimal distribution system (DS) planning with distributed generation (DG) systems. It is being done to see how active and reactive power injections affect the system's voltage profile and energy losses. DG penetration in the power systems is one approach that has several advantages such as peak savings, loss lessening, voltage profile amelioration. It also intends to increase system reliability, stability, and security. The main goal of optimal distributed generation (ODG) is a guarantee to achieve the benefits mentioned previously to increase the overall system efficiency. For extremely vast and complicated systems, analytical approaches are not suitable and insufficient. Therefore, several meta-heuristic techniques are favored to obtain better performance from were convergence and accuracy for large systems. In this paper, an Improved Wild Horse Optimization algorithm (IWHO) is proposed as a novel metaheuristic method for solving optimization issues in electrical power systems. IWHO is devised with inspirations from the social life behavior of wild horses. The suggested method is based on the horse's decency. To assess the efficacy of the IWHO, it is implemented on the 23 benchmark functions Reliability amelioration is the most things superb as a result of DGs incorporation. Thus, in this research, a customer-side reliability appraisal in the DS that having a DG unit was carried out by a Monte Carlo Simulation (MCS) approach to construct an artificial history for each ingredient across simulation duration. For load flow calculations, the backward Forward Sweep (BFS) technique has been employed as a simulation tool to assess the network performance considering the power handling restrictions. The proposed IWHO method has been measured on IEEE 33 69 and 119 buses to ascertain the network performing in the presence of the optimal DG and the potential benefits of the suggested technique for enhancing the tools used by operators and planners to maintain the system reliability and efficiency. The results proved that IWHO is an optimization method with lofty performance regarding the exploration–exploitation balance and convergence speed, as it successfully handles complicated problems.

1. Introduction

Nowadays, there is a global unanimity that incorporating renewable energy sources (RESs) as distributed generators (DG) is crucial to facing the rising electricity need and reducing the overall carbon dioxide footprint. It is one of the most successful and realistic planning methods for enhancing the network's reliability and power quality as demand increases. The DG penetration strategy in the DS is becoming more common as demand load increases, pollutant emissions are reduced, and the electrical power market is deregulated (Elattar and Elsayed, 2020). The leverage of DG performance is more closely related to the types, locations, and sizes of the DG units used, where the best choice will maximize the benefits of the DG units while avoiding their downsides for the system, such as voltage volatility, increased system loss and increased operating costs (Oree et al., 2017; Huda et al., 2017). The effects of including DG units into the system vary depending on whether the system is in steady-state or transient mode. Some issues occur in the steady-state, such

* Corresponding author at: Technological University Dublin, Dublin, Ireland.
E-mail addresses: Eng_MohammedHamouda@azhar.edu.eg (M.H. Ali), skamel@aswu.edu.eg (S. Kamel), mohamedhosnymoee@gmail.com (M.H. Hassan), mtostado@ujaen.es (M. Tostado-Véliz), hossam.zawbaa@gmail.com (H.M. Zawbaa).

https://doi.org/10.1016/j.egyr.2021.12.023

Nomenclature

I_i	The injected current at bus i
V_i	The injected voltage at bus i
S_i	Apparent power injections at the bus i
$Z_{(i,i+1)}$	The impedance of line $i, i+1$
R_i	The ith line resistance
P_i	Active power injections at the bus i
Q_i	Reactive power injections at the bus i
θ_{ij}	The admittance angle of line $i-j$
δ_j	The voltage angle at bus j
δ_i	The voltage angle at bus i
N	Number of buses
V_i^{min}	Minimum voltage at bus i
V_i^{max}	Maximum voltage at bus i
I_{li}	The line current flow of line i
I_{li}^{rated}	The rated line current capacity at line i
L	Energized number of branches
U_i	The annual outage time
N_i	The number of customers at load point i
L_i	The average load connected to load point i
it	Iteration
$maxit$	Maximum number of iterations
Γ	Gama function
P_{DG}^{min}	Minimum active power of DG capacity
P_{DG}	Active power of DG capacity
P_{DG}^{max}	Maximum active power of DG capacity
Q_{DG}^{min}	Minimum reactive power of DG capacity
Q_{DG}	Reactive power of DG capacity
Q_{DG}^{max}	Maximum reactive power of DG capacity
RDS	Radial distribution system
λ	Failure rate
U	Yearly unavailability
r	Outage time
$ASAI$	Average service availability index
$CAIDI$	Customer average interruption duration index
ENS	The energy not supplied index
hr	Hour
$MTTR$	Mean time to repair
$SAIFI$	System average interruption frequency index
$SAIDI$	System average interruption duration index
STD	Standard deviation
TTR	Time to repair
TTF	Time to failure
yr	Year

Abbreviation

AEO	Artificial ecosystem-based optimization
ALOA	Ant Lion Optimization Algorithm
AR	Automatic recloser
BA	Bat Algorithm
BFS	Backward Forward Sweep
BSOA	Backtracking search optimization algorithm
CSA	Cuckoo search algorithm
CBs	Circuit breakers
CPLS	Combined power loss sensitivity
DS	Distribution system
DG	Distributed generation
EA	Efficient analysis approach
ESDA	Electrostatic Discharge Algorithm
GA	Genetic algorithm
GS	Gauss-seidel
GWO	Gray Wolf Optimizer
HHO	Harris Hawks Optimizer
HGSO	Henry gas solubility optimization
HSSA	Hybrid Salp Swarm Algorithm
IA	Improved Analytical
IWHO	An improved wild horse optimization algorithm
LSF	Loss sensitivity factor
LSIPSO	Hybrid Loss Sensitivity Index and SA
MINLP	Mixed-integer nonlinear programming
MODE	Multi-objective differential evolution
MCS	Monte Carlo Simulation
NR	Newton raphson
OF	Objective function
ODG	Optimal distributed generation
PSO	Particle swarm optimization
PV	Photovoltaics
QOCSOS	Quasi-Oppositional Chaotic Symbiotic Organisms Search
RDG	Renewable distribution generation
RDN	Radial distribution network
RESs	Renewable energy sources
ROA	Rider optimization algorithm
SA	Simulated annealing
SAA	Simplified Analytical Approach
SAPSO	Hybrid SA and PSO
SAMPSO	Hybrid SA and modified PSO
SOA	Seagull Optimization Algorithm
SSA	Salp Swarm Algorithm
TSA	Tunicate Swarm Algorithm
WOA	Whale optimization algorithms
WT	Wind turbine

as extreme energy losses, reverse current flow, fluctuations in voltage, managing reactive power, malfunction in the protective system, and weak power quality (Baran et al., 2011; Dugan and Price, 2002; Walling et al., 2008). The consequences in the transitional state are, on the other hand, caused by the separating DG units and the unexpected outputs of the DG units, such as fluctuations in wind speed and solar radiation (Liu et al., 2008). The acuity of these effects is based on the placement of DG units, the DG penetration levels, and the sort of DG. Furthermore, due to renewable DG units' nature, simultaneous DG generation fluctuations for providing the demand load might lead to a down or overvoltage. The implications of such events may be altered by the placement of DG units and weather conditions, as mentioned previously (Eltawil and Zhao, 2010). Additionally, the system performance is enhanced at the particular penetration levels of the DG units, while the system was in contrast degraded by substation and feeder load, voltage deviations, and higher power losses

beyond this level. As a result, the ODG allocation problem has recently piqued the interest of many researchers to achieve various goals, including minimizing real power loss, enhancing voltage profile, boosting power quality, and mounting the distribution system's reliability and efficiency. As a result, many ways to address these issues have been proposed in the literature. A mixing of analytical approach and heuristic search has been suggested for optimal placement of DGs in the DS for minimizing power loss in Kansal et al. (2016). An efficient analysis (EA) approach to properly deploy multiple DG units is presented to reduce power loss in distribution systems (Mahmoud et al., 2015). A novel approach for determining the optimum size and the location of DG was presented in Essallah et al. (2019) to reduce the power loss and ensure the system's voltage stability. In Kadir et al. (2019), the authors used an enhanced gravitational search algorithm to learn the location and dimensions of photovoltaics (PV) based DGs to reduce overall expenditures. In Truong et al. (2020), the authors presented a technique that would increase the global seeking ability, called Quasi-Oppositional Chaotic Symbiotic Organisms Search (QOCSOS). The goal of this work is to curb the power loss, enhance the voltage profile, and raise the voltage stability in the radial distribution networks (RDNs). Mixed-integer nonlinear programming (MINLP) technique has been utilized in Kaur et al. (2014) to identify the best size and position of DGs with power loss curtailment. In Khasanov et al. (2019), the Electrostatic Discharge Algorithm (ESDA) was utilized to resolve the problem of DG assignment to augment the voltage stability and limit the power losses. To optimize the allocation of DGs in the DS concerning reducing annum power losses, the authors are introduced an artificial ecosystem-based technique (Khasanov et al., 2020). To decrease power loss in DS, a simplified analytical technique was presented for optimum DG amalgamation in Sa'ed et al. (2019). The aim of Kamel et al. (2019) is for an ODG allocation in the typical IEEE 33-bus system to promote voltage stability and minimize total power loss. This is based on the Gray Wolf optimization method with loss sensitivities. The Ant Lion Optimization Algorithm (ALOA) is presented in Ali et al. (2016) and Li et al. (2018) for ODG allocation of RDG sources in diverse RDNs. In Abdel-mawgoud et al. (2019), the authors offer a hybrid approach based on the combined power loss sensitivity (CPLS) and Salp Swarm Algorithm (SSA) to merge PV and wind turbines (WT) in the DS for boosting voltage, reducing losses, and expanding system capacity. The purpose of Samala and Kotapuri (2020) is to resolve the best allocation of the DGs in a RDN, diminish the overall operational costs and voltage indexes variations, and ensure a more flexible solution of the hybrid fuzzy logic controller technique and the particle swarm optimization (PSO) with the ALOA. The authors utilized the LSF in Ali et al. (2020b,a) to locate the elected bus. To mend the voltage profile and decrease the power loss of the RDN, simulated annealing (SA) and PSO were used to set the optimal position and size of DG. The SAPSO approach to banning the SA & PSO shortage by two methods was introduced and produced the finest solutions in a short time. This article (Khasanov et al., 2021; Hassan et al., 2020a) provides an application for optimal sizing and positioning of RDGs, including WT, PV, and biomass in DS. The goal of the study in Ref. Hassan et al. (2020b) was to find the best position and size for DGs to reduce power loss and increase voltage stability.

To epitomize, an improved wild horse optimization algorithm (IWHO) is suggested as a novel population-based algorithm to compete with state-of-the-art and neoteric optimization algorithms. It should be evident that the intended algorithm provides the poise between exploration and exploitation. This feature enables IWHO to solve a complicated optimization issue with multiple locally optimal solutions because it retains several answers and explores a broad area to pinpoint the global solution. Finally, the IWHO is the greatest and most innovative approach for optimizing problems because of loud fineness and soft calculations. To sum up, this research's key contributions are:

The benchmark functions of various types of unimodal, multimodal, and fixed-dimensional composite functions is utilized to evaluate the proposed improved wild horse optimization algorithm (IWHO) efficiency.

Introduce for the first time in the power system a devised approach to augment search quality and shun an early convergence to a local minimum.

Proposed the optimal option of the ODG allocation (size & position) considering the constraints of the RDN. Standard IEEE 33, 69 and 119 bus networks are hired to check the leverage of the suggested IWHO algorithm.

Demonstrated the efficacy of the outcomes of this approach in terms of lowering losses and meliorative the voltage profile.

Verified the methodology's performance proposed using typical test systems to detect its superiority for handling the problems and compared to other published approaches.

An artificial history for each component in the test system is generated using MCS instead of an analytical method for highly efficient reliability assessment.

This paper was structured as follows: Section 2 depicts the BFS algorithm. The mathematical description of the optimization problem is described in Section 3. Section 4 focuses on the IWHO algorithm. Section 5 transact with the simulation results for the test systems and discussion. Finally, in Section 6, the suggested work's inference is provided.

2. Backward forward sweep algorithm

Load flow is a crucial tool for the design and operation of power systems to guarantee reliability, stability, and economy. Classical methods as Gauss–Seidel (GS) and Newton Raphson (NR) might be inappropriate for the DS and diverge because of Ali et al. (2020a):

- Radial formation.
- R/X value is higher.
- Running lopsided.
- DGs.

Backward/Forward Sweep (BFS) is chosen for fit planning owing to:

- The poor nature of RDS.
- Accurate load flow results rely on convergence, simulation time, and the convergence rate.

This technique is carried out through two phases: rear and front sweep using the demand and streak data as follow:

2.1. Forward sweep

In essence, a voltage decline is calculated through branch currents. Node voltages are updated from the first bus to the most distant bus. The fore scanning aims to identify the node voltage for all buses starting from the origin node. The primary bus voltage is set to 1pu, and the current in reverse propagation is firm.

2.2. Backward sweep

It is mainly a voltage upgraded by a load flow computation. It moves from the furthest lines to the head node. In the rear-prevalence count, the updated current flows are achieved utilizing the bus voltage of the previous rounds. It implies that the voltage values obtained are not changed during the rear prevalence computations in the front prevalence.

The BFS algorithm steps are listed below:

- Set the injected current ($I_i = 0$)
- Set all nodes voltage ($V_i = 1pu$)
- Compute the node current ($I_i = \frac{S_i^*}{V_i^*}$)
- Evaluate current of the lines (backward sweep)

$$I_{(i,i+1)} = I_{i+1} + \sum(\text{branches current at node } i+1)$$

- Modernizing the voltage of buses ($V_i = V_{i+1} + (Z_{(i,i+1)} * I_{(i,i+1)})$)
- Until the criteria are terminated.

3. Problem formulation

The main key for a healthy environment is renewable distribution generation (RDG), which plays a main role in power systems. Tentatively, the peril of fuel price swings and political influences should be decreased by incorporating the RDGs and guaranteeing that these do not significantly influence public well-being overall. In such regard, changes to the grid might be necessary due to modifying the choices of generating sources, which is caused by a large amalgamation of RDGs. The fluctuation of current and voltage in the network is increased as a result of DG permeation. Increasing DG permeation might therefore have a detrimental or beneficial influence depending on the scale of the system and the sort of the load, necessitating modeling and emulation to evaluate its action. If not adequately striped, this may result in an unforeseen rise in power flow, leading to network crowding and higher network losses. DGs offer terminus consumers significant advantages and technical assistance through increased reliability, power quality, and cost dilution. Cost cuts and the pressing requirement to fuse DGs maybe drive energy demand. Therefore, good system planning is significant for the good running of the entire system. This concerns the development of convenient mathematical models and algorithms that allow for optimum positioning and size of DGs in the system; this is the issue handled in this study.

3.1. Objective Function (OF)

Its major aim is to identify the best localization and sizing of DGs to constrict the total losses in light of equity and inequality restrictions., which can be described as follow:

$$OF = min\,(P_{loss}) = min \sum_{i=1}^{L} R_i\left(\frac{P_i^2 + Q_i^2}{V_i^2}\right) \tag{1}$$

3.2. Constraints

The limits ensuring the superior performance of the RDGs technology are split into operating and technological restrictions as see:

3.2.1. Operational constraints

These are called the equality restriction and apportioned into:

- Power balance constraints

$$P_i = |V_i| \sum_{j=1}^{N} \left|V_j\right| \times \left|Y_{ij}\right| \times \cos\left(\theta_{ij} + \delta_j - \delta_i\right), \forall i \in N \tag{2}$$

$$Q_i = -|V_i| \sum_{j=1}^{N} |V_j| \times |Y_{ij}| \times \sin(\theta_{ij} + \delta_j - \delta_i), \forall i \in N \tag{3}$$

3.2.2. Technical constraints

These are called the inequality restriction and apportioned into:

- Voltage constraints

$$\left|V_i^{min}\right| \le |Vi| \le \left|V_i^{max}\right|, \forall i \in N \tag{4}$$

- Current constraints

$$I_{li} \le I_{li}^{rated}, \forall i \in L \tag{5}$$

- DG size constraints

$$P_{DG}^{min} \le P_{DG} \le P_{DG}^{max} \tag{6}$$

$$Q_{DG}^{min} \le Q_{DG} \le Q_{DG}^{max} \tag{7}$$

- DG location constraints

$$2 \le DG_{location} \le N_{bus} \tag{8}$$

where L is the energized number of branches; N is the number of buses; Y_{ij} is the bus admittance of line i-j; θ_{ij} is the admittance angle of line i-j; $\left|V_i^{min}\right|$; $\left|V_i^{max}\right|$ are the limits of the voltage at the bus i; I_{li} is the line current flow of line i; I_{li}^{rated} is the rated line current capacity at line i.

3.3. Reliability assessment for distribution systems

The measurement of reliability is a crucial agent for the planning and operation of DS. Based on system configuration and item's reliability data, DS reliability evaluation may forecast the obstruction of a DS at the client end. The primary goal of reliability analysis is to measure, forecast, and compare reliability indicators for multiple network topologies for reliability rising. The reliability evaluation calculates performance at client load points while factoring in the stochastic nature of failures incidence and outage period. The main indicators linked with client points are failure rate (λ), outage time (r), and yearly unavailability (U), which may be computed using Eqs. (9)–(10).

$$\lambda_p = \sum_{i=1}^{N} \lambda_i \left(\frac{f}{yr}\right) \tag{9}$$

$$U_p = \sum_{i=1}^{N} \lambda_i r_i \left(\frac{hr}{yr}\right) \tag{10}$$

$$r_p = \frac{U_p}{\lambda_p}\,(hr) \tag{11}$$

3.3.1. Monte-Carlo Simulation approach

Because a power system is uncertain, the Monte-Carlo simulation approach may be used to provide more exact findings when evaluating its reliability. Monte-Carlo simulation can be classified into two types: time-sequential and state sampling methods, but the time-sequential technique is utilized here.

State of the basic distribution equipment such as branches, transformers, and protective components such as disconnecting switches, breakers, and fuses helps for system reliability valuation. In general, line segments and transformers may be depicted by two states seen in Fig. 1, where the upstate signifies that the portion is operational and the downstate shows that the portion is dud.

The time to failure is the period that the item persists in the upper (TTF) or failure time (FT), But the period, while an element is down, is called a reconquest time and it might be either the time to repair (TTR) or the time to substitute. The transition from the up to down is the failure operation, while the transition from down to up is the restoration operation. Fig. 2 depicts the history of simulated element operation and repair.

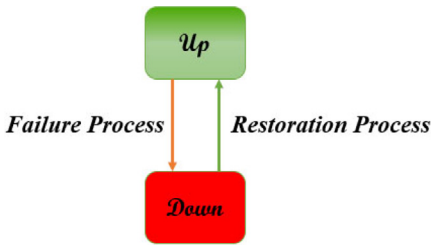

Fig. 1. Element state transition diagram.

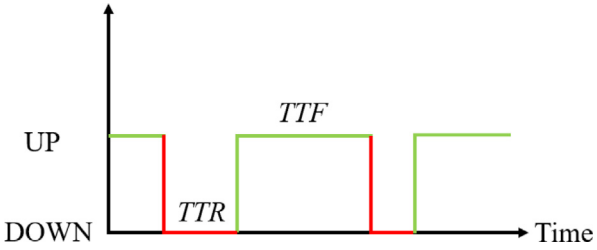

Fig. 2. Component Up/Down history.

TTF and *TTR* are randomly generated with potentially varying probabilistic. A universal random number generator can create a uniform distribution direct, and the resulting random numbers are transformed into *TTF* or *TTR* using these formulas.

$$TTF = \left(-\log\frac{U}{\lambda}\right) * 8760 \tag{12}$$

$$TTR = -\log U * MTTR \tag{13}$$

where U is a haphazard variable in the range [0, 1].

3.3.2. Load point failures identification

The harshest issue in the emulation is to detect the load points influenced by the fiasco of an element. A complicated RDN can be broken down into primary feeders and laterals. The following is the technique for detecting failing load points and their operation/restoration histories (Billinton and Wang, 1999):

1. Discover the failure object and its location, as well as the failed elements number and the lost feeder's amount to which the failed element is linked.
2. Identify the impacted load points that are linked to the failing feeder, as well as their failure intervals, based on the setup and protection system of the damaged feeder.
3. Determine the downstream feeders linked to the damaged feeder's sub-feeders and the impact of the damaged component on the load points linked to these sub-feeders.
4. Repeat steps 2 and 3 for every failing sub-feeder till all sub-feeders linked to the failing feeder are identified and analyzed.
5. Find the upstream feeder to which the failing feeder is linked, as well as the impacts of the failure component on the load points in the upstream feeder.
6. Reiterate (2) to (5) until the primary feeder is reached and assessed.

The client obstruction indicators will be used to quantify system reliability; the main indicators are the customer average interruption duration index (*CAIDI*), the system average interruption frequency index (*SAIFI*), the system average interruption duration index (*SAIDI*), the average service availability index (*ASAI*), and the energy not supplied index (*ENS*). The following equations are used to compute them (Transmission et al., 2003):

$$SAIFI = \frac{\sum_{i=1}^{k}\lambda_i N_i}{\sum_{i=1}^{k} N_i} \tag{14}$$

$$SAIDI = \frac{\sum_{i=1}^{k} U_i N_i}{\sum_{i=1}^{k} N_i} \tag{15}$$

$$CAIDI = \frac{\sum_{i=1}^{k} U_i N_i}{\sum_{i=1}^{k}\lambda_i N_i} = \frac{SAIDI}{SAIFI} \tag{16}$$

$$ASAI = \frac{\sum_{i=1}^{k} 8760\, N_i - \sum_{i=1}^{k} U_i N_i}{\sum_{i=1}^{k} 8760\, N_i} \tag{17}$$

$$ENS = \sum_{i=1}^{k} U_i L_i \tag{18}$$

where U_i is the annual outage time, N_i is the number of customers at load point i, λ_i is the failure rate, and "L_i" is the average load connected to load point i and 8760 is the number of hours in a calendar year.

The developed flow chart of the computer program to determine the distribution system reliability indices consists of the following steps: (see Fig. 3).

4. Mathematical model of optimization techniques

4.1. Wild horse optimizer (WHO)

For addressing optimization issues, the wild horse optimizer (WHO) technique mathematically simulates and duplicates the social life behavior of these wild horses in nature (Naruei and Keynia, 2021). Horses predominately live in herds with a stallion and many foals and mares. They exhibit a variety of behaviors, including mating and grazing, pursuing, dominating, commanding. Five steps for the WHO algorithm are listed below:

4.1.1. Generating an initial population and formation horse groups and choosing leaders

First, the initial population is divided into numerous groups. N is the number of the population and G is the number of groups in the algorithm. Each group has a leader (stallion), so the number of stallions in the algorithm equals G, and (N–G) is the remaining population (Foals and mares) are distributed similarly among these groups. Fig. 4 presents how the stallions and foals have been chosen from the initial population to produce various groups.

4.1.2. Grazing behavior

The following equation was proposed to simulate the grazing behavior:

$$X_{i,G}^{j} = 2Z\cos(2\pi RZ) \times \left(Stallion^{j} - X_{i,G}^{j}\right) + Stallion^{j} \tag{19}$$

where $X_{i,G}^{j}$ denotes the current location of the foal or mare group member, $Stallion^{j}$ is the stallion position, R is a uniform stochastic number from the range [−2,2], and Z is the adaptive mechanism calculated from the following equation:

$$P = \overrightarrow{R_1} < TDR; \qquad IDX = (P == 0);$$
$$Z = R_2 \Theta IDX + \overrightarrow{R_3}\Theta(\sim IDX) \tag{20}$$

where P is a vector consisting of 0 to 1, $\overrightarrow{R_1}$ and $\overrightarrow{R_3}$ are a random number from the range [0,1], R_2 is a uniform random number from the range [0,1]. *TDR* is an adaptive parameter that starts with 1 and decreases until it reaches 0 at the end of the implementation of the algorithm according to the following equation:

$$TDR = 1 - it \times \left(\frac{1}{maxit}\right) \tag{21}$$

where it is the current iteration and $maxit$ is the maximum number of iterations.

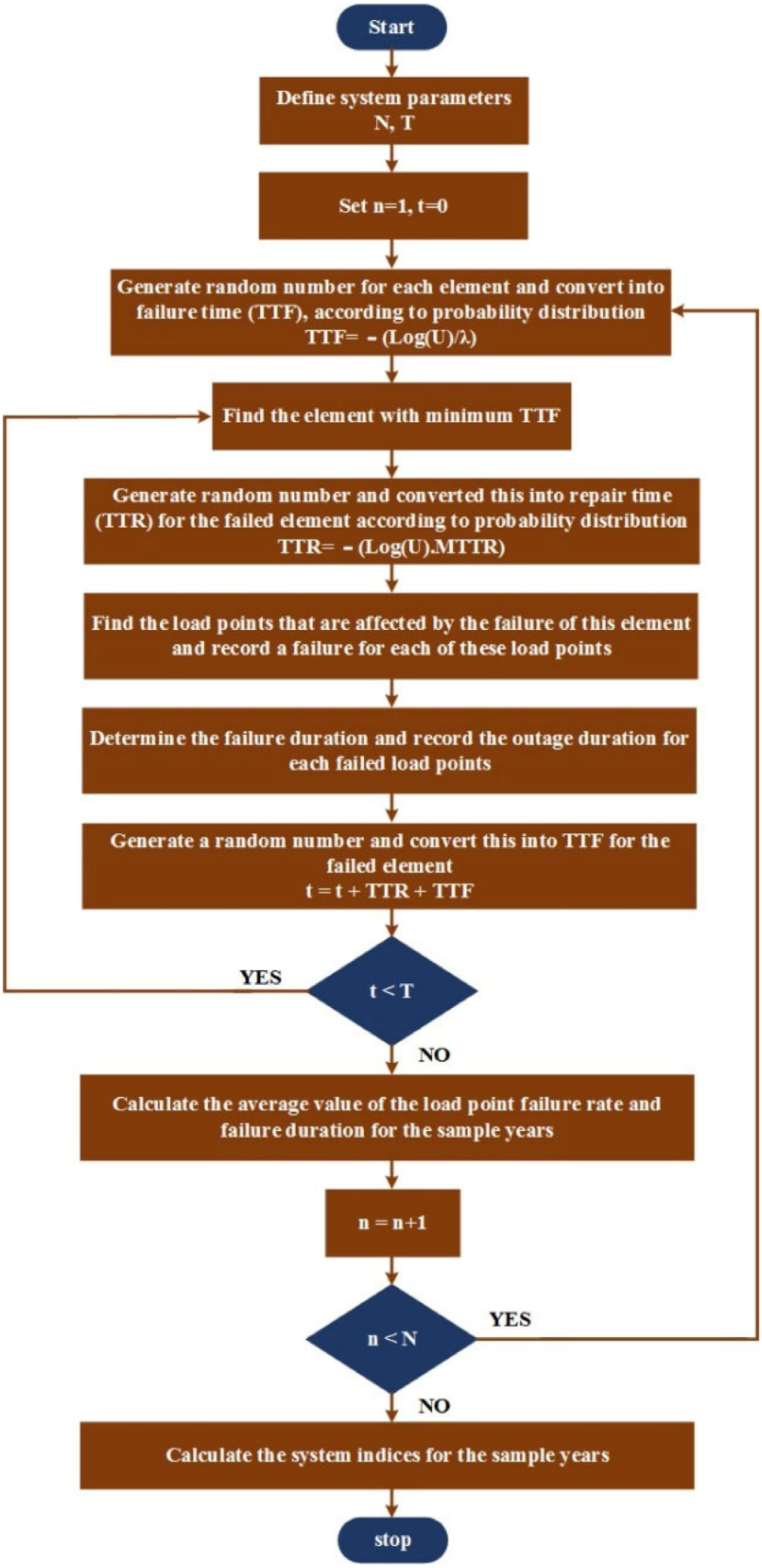

Fig. 3. Flowchart for Monte Carlo simulation.

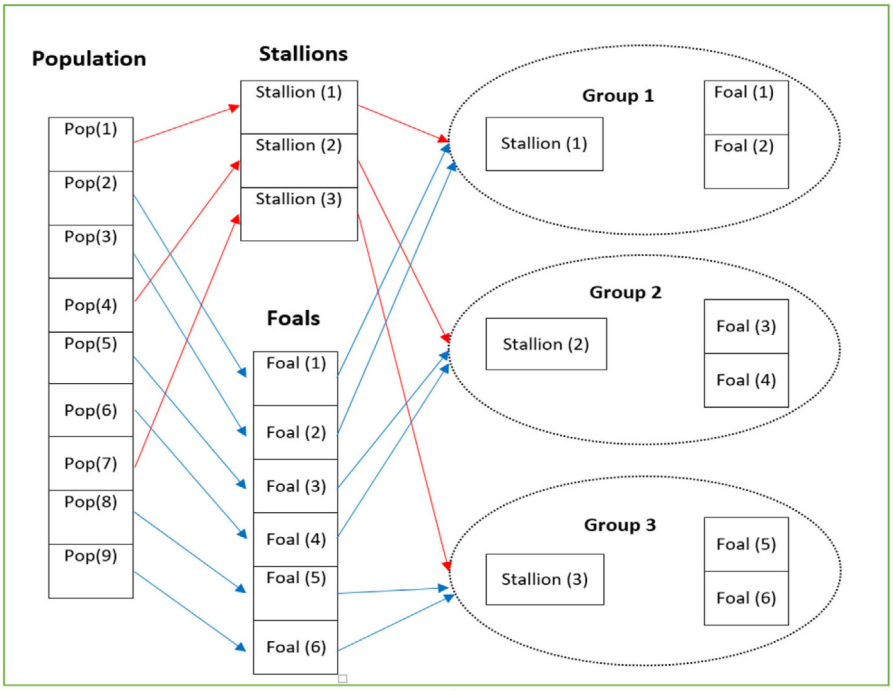

Fig. 4. Formation of groups from the original population.

4.1.3. Horse mating behavior

To implement the mating behavior of horses, a foal goes from group i to a temporary group while a foal goes from group j to a temporary group. To simulate the mating behavior of horses, the Crossover operator of the mean type was proposed as follows:

$$X_{G,K}^{P} = Crossover\left(X_{G,i}^{q}, X_{G,j}^{z}\right) i \neq j \neq k, p = q = end,$$
$$Crossover = Mean \tag{22}$$

4.1.4. Group leadership

In the WHO algorithm, the Stallions (group leaders) lead the group to the water hole. The Stallions compete for this water hole so that the domination group can employ this water hole firstly and then other groups can use the water hole. The following equation was recommended for this step of the algorithm:

$$\overline{Stallion_{G_i}} = \begin{cases} 2Z\cos(2\pi RZ) \times \left(WH - Stallion_{G_i}\right) \\ +WH \ if \ R_3 > 0.5 \\ 2Z\cos(2\pi RZ) \times \left(WH - Stallion_{G_i}\right) \\ -WH \ if \ R_3 \leq 0.5 \end{cases} \tag{23}$$

where $\overline{Stallion_{G_i}}$ is the next position of the leader. WH is the location of the water hole.

4.1.5. Leaders interchange and selection

In the following stages, leaders are chosen according to fitness. The leader position and the relevant member will change based on this equation:

$$\overline{Stallion_{G_i}} = \begin{cases} X_{G,i} \ if \cos t(X_{G,i}) < \cos t(Stallion_{G_i}) \\ Stallion_{G_i} \ if \cos t(X_{G,i}) > \cos t(Stallion_{G_i}) \end{cases} \tag{24}$$

Fig. 5 presents the flow chart of WHO algorithm.

4.2. Improved Wild horse optimizer (IWHO)

The Improved Wild horse optimizer (IWHO) is based on the cuckoo search (CS) algorithm (Gandomi et al., 2013). During the iteration of the proposed algorithm, the new solution is generated using the Levy flight as the following equation:

$$X_{i,G} = X_{i,G} - \gamma\left(X_{i,G} - X_g\right) \oplus Levy(\lambda) = X_{i,G} + \frac{0.01u}{|v|^{1/\lambda}}\left(X_{i,G} - X_g\right) \tag{25}$$

where $X_{i,G}$ is the ith position of the group member, γ denotes the step scaling size, X_g denotes the global best solution, the $\oplus$ refers to the process of element-wise multiplications, λ refers to the Levy flight exponent, while u and v are defined as:

$$u \sim N\left(0, \sigma_u^2\right), v \sim N\left(0, \sigma_v^2\right) \tag{26}$$

The standard deviations σ_u and σ_v are expressed as:

$$\sigma_u = \left[\frac{\sin\left(\frac{\lambda\pi}{2}\right).\Gamma(1+\lambda)}{2^{(\lambda-1)}\lambda.\Gamma\left(\frac{1+\lambda}{2}\right)}\right]^{1/\lambda}, \sigma_v = 1 \tag{27}$$

where Γ is the Gamma function, the new candidate solution is generated, and Eq. (21) is applied. The principal advantage of this improvement is the ability of the proposed technique to balance global exploration and local exploitation (Long et al., 2020). Finally, it has the same concept as in Ref. Zhang et al. (2015) that to address the issue of faster convergence by using a mutation strategy based on the GA. Fig. 6 shows the flow chart of the IWHO algorithm.

5. Simulation results and discussion

5.1. Mathematical validation

To evaluate the robustness of the suggested IWHO algorithm, it was run separately on all 23 OFs for the maximum iterations number of 1000 and the agents' number of 50. To assess the algorithm's performance, this research uses both quantitative and qualitative measures. Fig. 7 shows the qualitative metrics for some of the benchmark functions, including 2D views of the functions, search histories, mean fitness histories, and convergence curves.

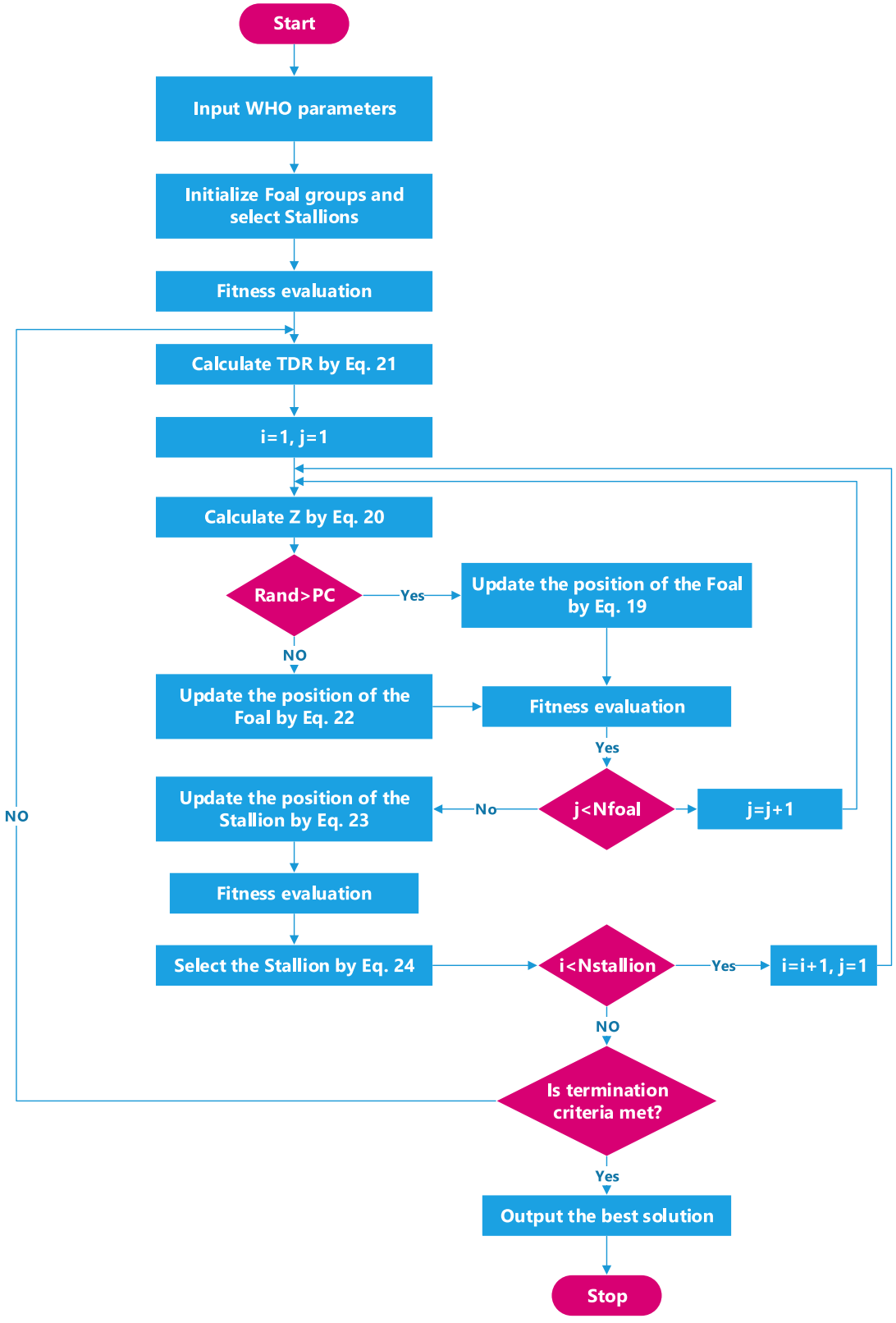

Fig. 5. The flow chart of WHO algorithm.

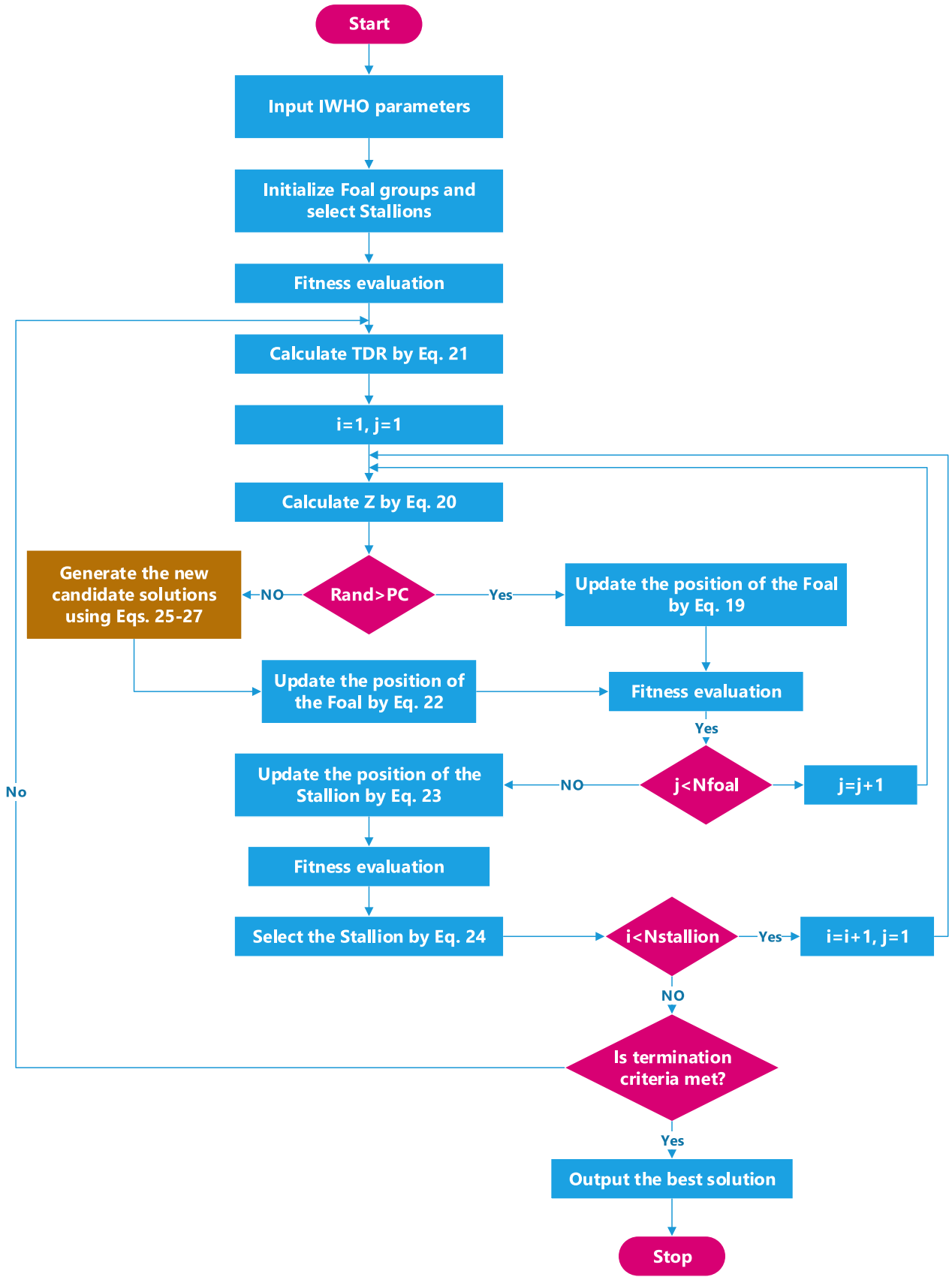

Fig. 6. The flow chart of IWHO algorithm.

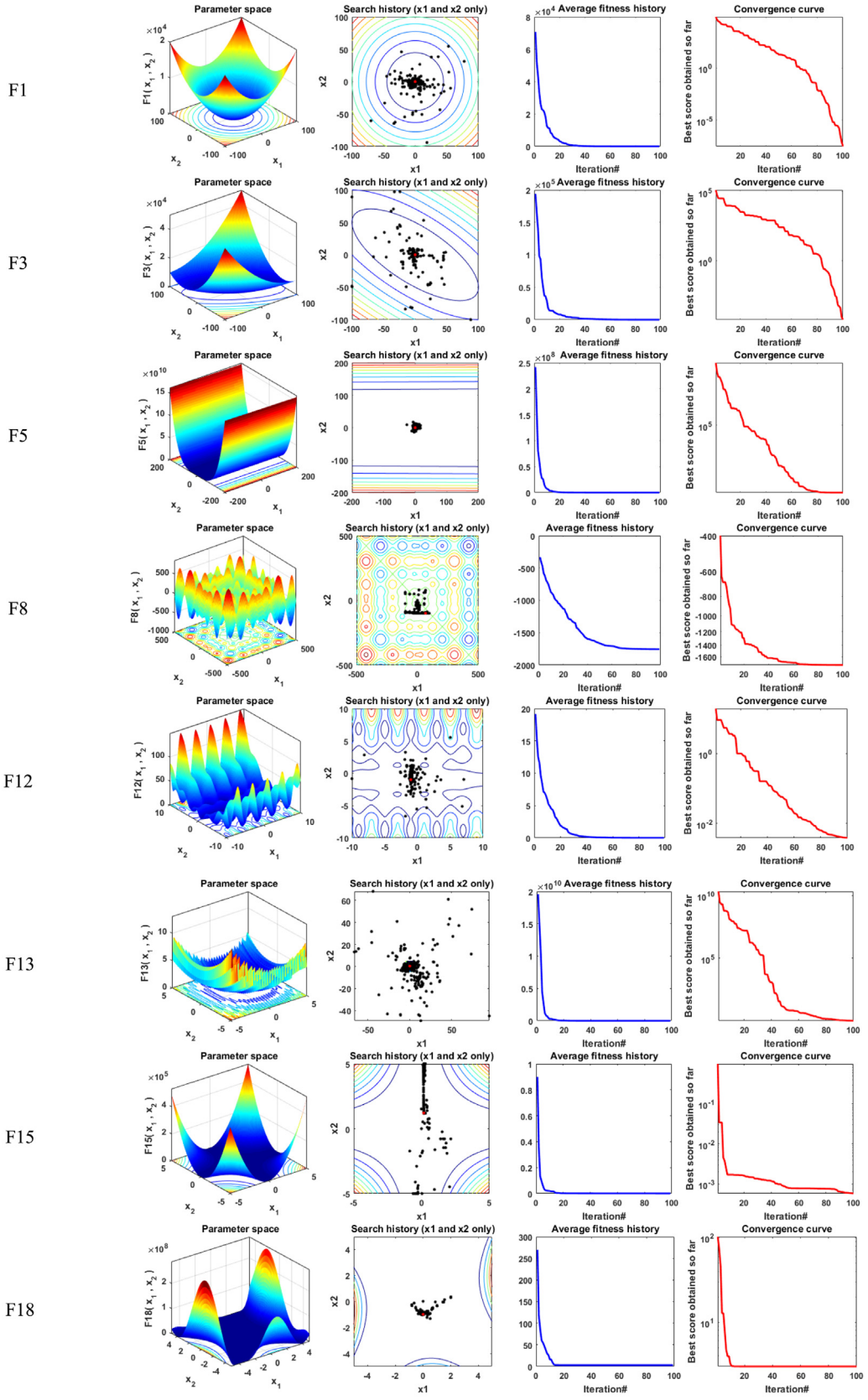

Fig. 7. Qualitative metrics on some benchmark functions: 2D views of the functions, search history, mean fitness history, and convergence characteristics curve.

Table 1
Parameter sets of the chosen algorithms.

Algorithms	Parameters setting
Common settings	Population size: nPop = 50 Maximum iterations : Max_iter = 1000 Number of separate runs: 20
SOA	b = 1
IWHO	PS = 0.2; % Stallions percentage
WHO	PC = 0.13; % Crossover percentage

Also, the suggested IWHO was tested for its ability to provide a quasi-suitable solution on a collection of 23 objective functions of various types of unimodal, multi-modal, and fixed-dimensional composite functions (Dehghani et al., 2021). The obtained results are compared with three recent algorithms Gray Wolf Optimizer (GWO) algorithm (Mirjalili et al., 2014), Tunicate Swarm Algorithm (TSA) (Kaur et al., 2020), and Seagull Optimization Algorithm (SOA) (Dhiman and Kumar, 2019), as well as the original WHO. The parameter setting of the chosen algorithms is shown in Table 1. Each optimization technique was executed in 20 independent runs; the optimization results are presented as the best, worst, average, and the standard deviation (std) of the preferable solutions, respectively.

5.1.1. Evaluation of the objective functions findings for unimodal

The suggested algorithm's exploitative capacity may be assessed and evaluated using the unimodal test functions. Table 1 displays the best values achieved using the proposed and well-known optimization algorithms for these benchmark functions. It can be noticed that the IWHO technique provides better results on all unimodal functions except F7 which the original WHO reaches only for the best answer while the proposed algorithm achieves the best values for it in the worst, mean, and std. The suggested IWHO method produces better results than existing approaches for all unimodal test functions. Fig. 8 depicts the convergence characteristics curves of the introduced IWHO approach, including well optimization techniques for unimodal benchmark functions. For more analysis to confirm the performance of the recommended technique, a boxplot of outcomes for each technique and OF is demonstrated in Fig. 9.

5.1.2. Evaluation of the objective functions findings for multi-modal

Six objective functions of multi-modal functions, including F8 to F13, were chosen to evaluate the performance of the proposed IWHO technique in presenting the best solutions. The results of the implementation of the IWHO algorithm and three other optimization algorithms as well as the conventional WHO algorithm on this type of objective function, are displayed in Table 2. The emulation results prove that the IWHO performs better and more competitively in tackling this sort of optimization issue. Fig. 10 displays the convergence curves of IWHO and other rival methods. Fig. 11 presents the box plot for the proposed IWHO and other concurrent algorithms on multi-modal functions. According to the results, the proposed IWHO technique is the greatest optimization technique for the majority of the evaluation metrics.

5.1.3. Evaluation results on composite objective functions

Ten objective functions of composite functions, including F14 to F23, were chosen to assess the performance of the proposed IWHO in providing optimal solutions. Table 3 presents the best optimum solutions found by all algorithms, including the best, worst, average, and STD. Fig. 12 displays the convergence curves of the proposed IWHO technique and other techniques achieved in the multiple benchmark functions. Fig. 13 displays the boxplots for F14 to F23. It can be seen that the boxplots of the proposed IWHO when compared to other techniques, are highly tight for the majority of these functions with the lowest values (see Table 4).

Table 2
Benchmark function outcomes for unimodal.

Function		WHO	IWHO	GWO	TSA	SOA
F1	Best	2.6E−115	**8.2E−121**	1.6E−72	2.82E−55	4.76E−30
	Worst	9.5E−106	**1.4E−108**	3.42E−07	3.45E−17	5.06E−10
	Mean	1.1E−106	**6.9E−110**	1.71E−08	1.72E−18	2.53E−11
	Std	2.8E−106	**3.1E−109**	7.65E−08	7.71E−18	1.13E−10
F2	Best	1.53E−65	**1.18E−66**	5.52E−29	6.19E−27	1.3E−17
	Worst	1.03E−59	**2.14E−61**	4.4E−08	7.35E−13	4.26E−08
	Mean	2E−60	**1.49E−62**	2.39E−09	3.68E−14	2.15E−09
	Std	3.17E−60	**4.81E−62**	9.81E−09	1.64E−13	9.52E−09
F3	Best	1.95E−77	**3.99E−83**	2.22E−14	6.22E−12	4.12E−16
	Worst	6.75E−64	**3.47E−68**	1.200307	195.9186	0.54897
	Mean	4.99E−65	**1.75E−69**	0.175247	24.31458	0.039322
	Std	1.63E−64	**7.76E−69**	0.401434	60.03018	0.124825
F4	Best	4.83E−46	**6.5E−50**	1.7E−13	0.004211	1.88E−08
	Worst	4.2E−41	**1.16E−42**	0.123216	21.22892	1.489819
	Mean	4.68E−42	**7.93E−44**	0.012534	3.538218	0.21736
	Std	1.18E−41	**2.63E−43**	0.037861	6.441649	0.523316
F5	Best	23.62242	**23.06539**	26.41102	27.10919	27.20026
	Worst	28.53885	**24.57677**	28.93196	28.92147	28.93044
	Mean	24.46879	**24.07834**	27.85099	28.38438	28.54089
	Std	1.000308	**0.415118**	0.799818	0.675004	0.57121
F6	Best	2.19E−18	**1.78E−18**	0.249992	2.596274	2.507228
	Worst	2.92E−14	**2.84E−15**	6.754946	6.30706	6.133702
	Mean	2.04E−15	**4.52E−16**	2.39919	4.176579	4.253747
	Std	6.58E−15	**7.79E−16**	1.752866	1.013975	1.034333
F7	Best	**6.26E−05**	9.83E−05	0.000439	0.005675	0.000389
	Worst	0.00123	**0.00078**	0.008863	0.052199	0.024776
	Mean	0.000421	**0.000293**	0.00327	0.014535	0.006081
	Std	0.00027	**0.000162**	0.002825	0.010611	0.006765

The best values obtained are in bold.

Table 3
Benchmark function outcomes for multi-modal.

Function		WHO	IWHO	GWO	TSA	SOA
F8	Best	−10331.3	**−10867.3**	−6876.85	−6687.08	−5688.53
	Worst	−8811.26	**−8909.96**	−2040.64	−3353.87	−3025.17
	Mean	−9512.65	**−9654.44**	−5363.86	−5404.01	−4662.31
	Std	**377.1542**	469.3701	1298.089	964.0392	721.2641
F9	Best	**0.00E+00**	**0.00E+00**	**0.00E+00**	101.0783	**0.00E+00**
	Worst	**0.00E+00**	**0.00E+00**	10.64299	312.5106	19.6612
	Mean	**0.00E+00**	**0.00E+00**	1.088214	196.4102	2.489027
	Std	**0.00E+00**	**0.00E+00**	2.989658	51.77915	5.370562
F10	Best	**8.88E−16**	**8.88E−16**	2.22E−14	1.51E−14	19.95954
	Worst	**4.44E−15**	**4.44E−15**	4.94E−07	2.891204	19.96677
	Mean	3.2E−15	**3.02E−15**	2.56E−08	0.545612	19.96242
	Std	**1.74E−15**	1.79E−15	1.1E−07	1.123192	0.001919
F11	Best	**0.00E+00**	**0.00E+00**	**0.00E+00**	**0.00E+00**	**0.00E+00**
	Worst	**0.00E+00**	**0.00E+00**	0.034439	0.151418	0.11477
	Mean	**0.00E+00**	**0.00E+00**	0.003728	0.029085	0.013796
	Std	**0.00E+00**	**0.00E+00**	0.009503	0.052147	0.033163
F12	Best	8.23E−20	**2.12E−20**	0.035117	0.478781	0.237936
	Worst	**0.103669**	0.207317	1.373427	18.46794	1.633411
	Mean	**0.010367**	0.020732	0.253217	6.960091	0.619033
	Std	**0.031909**	0.063811	0.394467	5.091209	0.411038
F13	Best	**1.2E−18**	1.1E−17	0.569956	1.889159	1.854413
	Worst	**0.109867**	0.175786	2.764004	3.467599	2.898385
	Mean	**0.019212**	0.034458	1.354047	2.824032	2.29935
	Std	**0.028468**	0.050856	0.672746	0.437644	0.298225

The best values obtained are in bold.

5.2. Test systems

The described algorithm was employed and validated on IEEE 33 and 69-bus networks to ensure its usefulness. The starting node voltage is assumed to be 1pu, and all loading buses are considered viable installation options. MATLAB 2020b software was used to perform the suggested technique utilizing Intel(R)

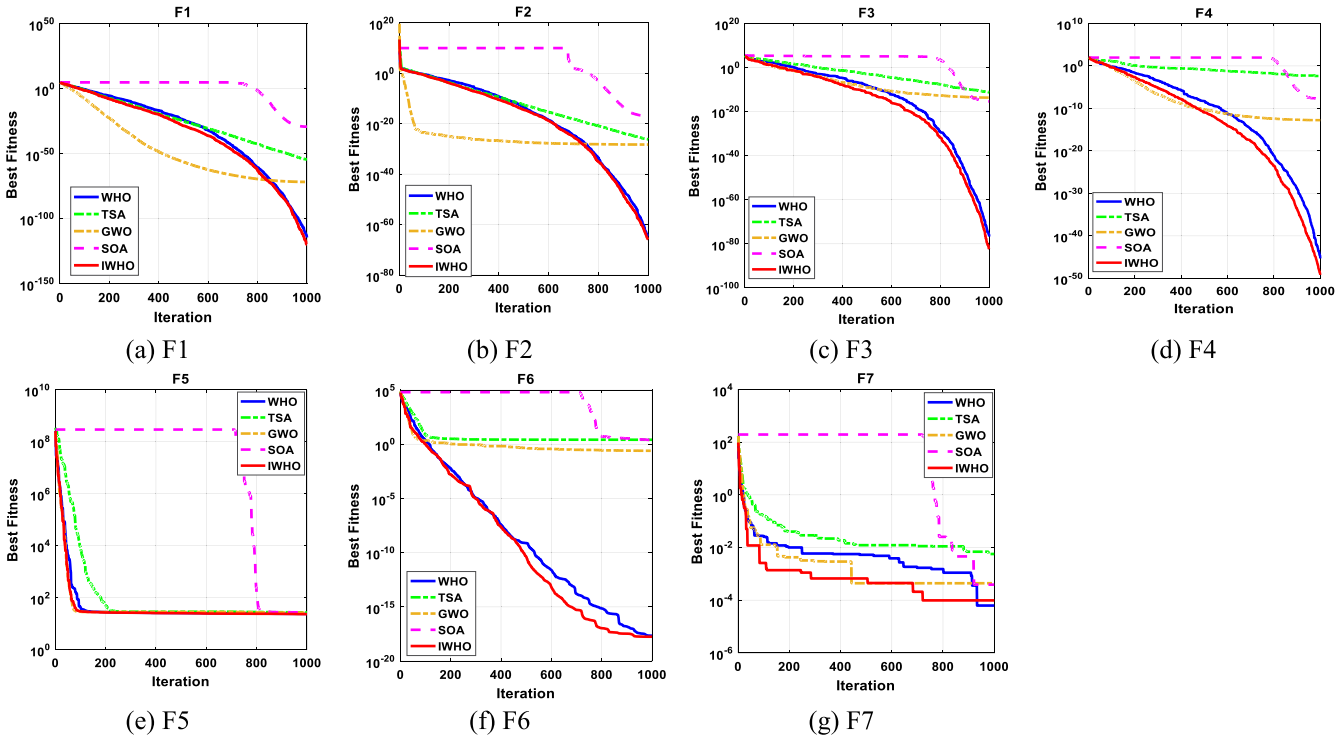

Fig. 8. The convergence curves of all algorithms for unimodal benchmark functions.

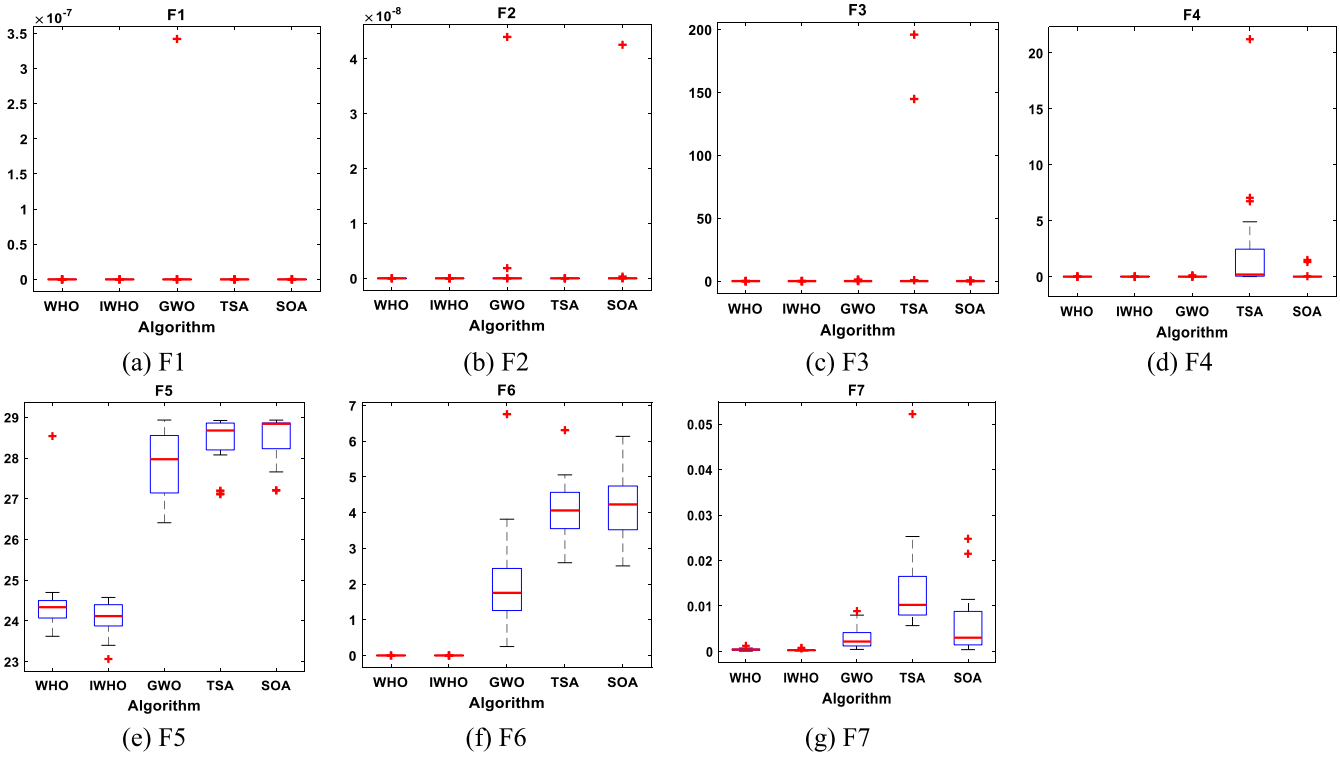

Fig. 9. Boxplots for all algorithms for unimodal benchmark functions.

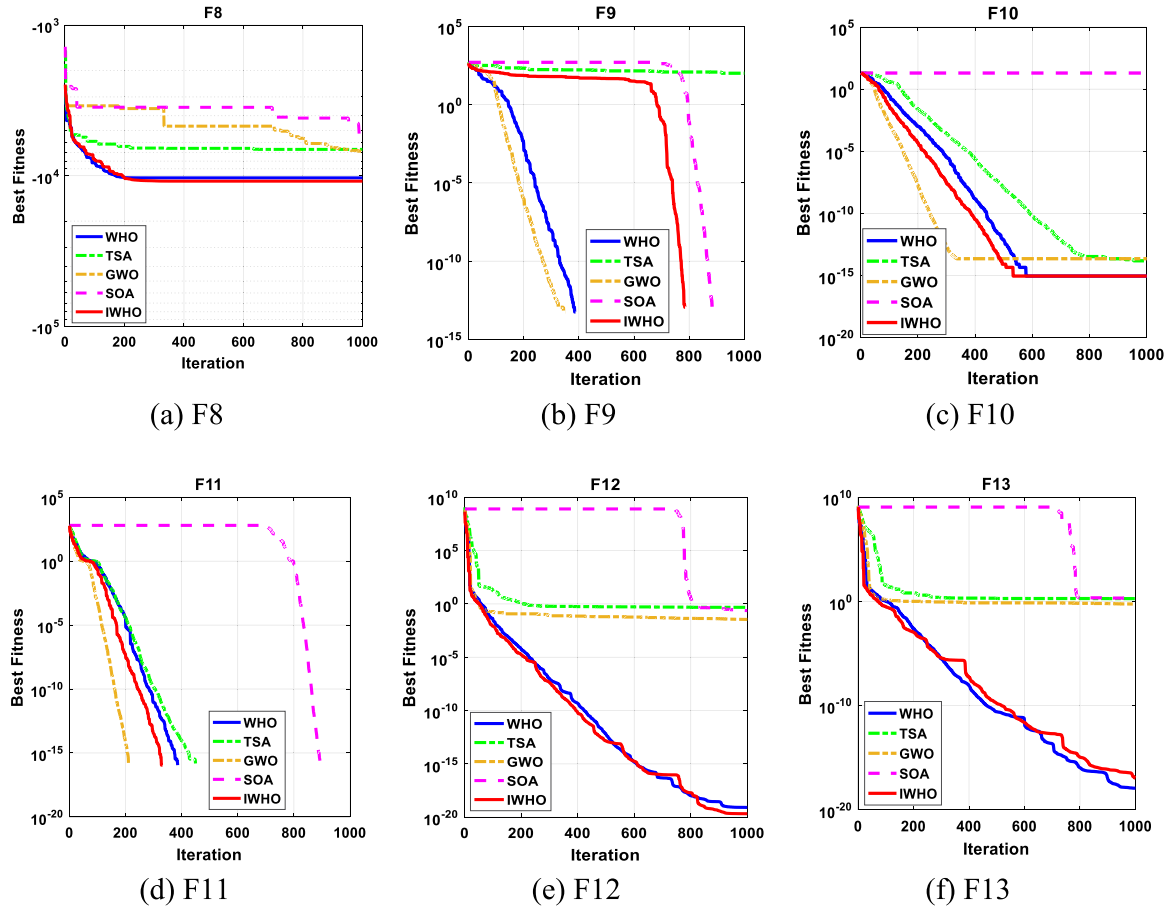

Fig. 10. The convergence curves of all algorithms for multi-modal benchmark functions.

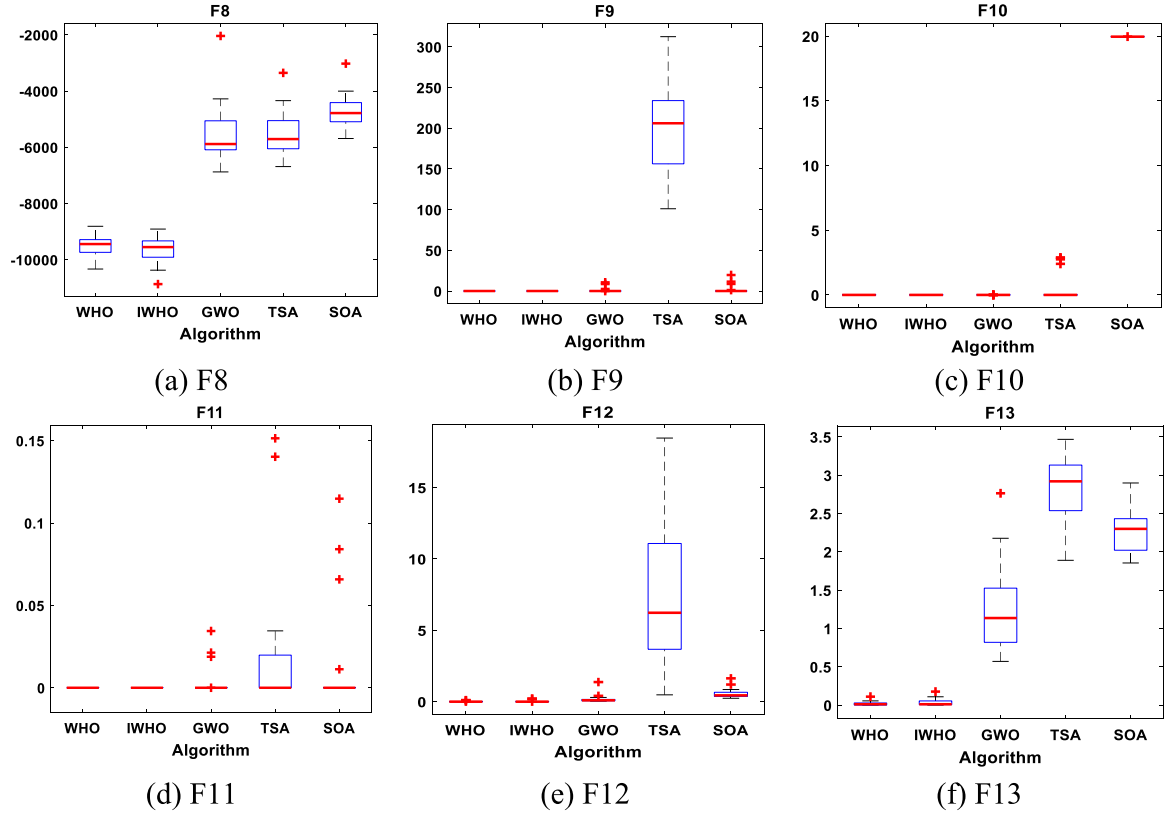

Fig. 11. Boxplots for all algorithms for multi-modal benchmark functions.

Table 4
Results of composite benchmark functions.

Function		WHO	IWHO	GWO	TSA	SOA
F14	Best	**0.998004**	**0.998004**	**0.998004**	**0.998004**	**0.998004**
	Worst	5.928845	**2.982105**	12.67051	12.67051	12.67051
	Mean	1.294247	**1.14691**	5.686485	7.493557	4.423671
	Std	1.113224	**0.485651**	4.930301	4.617822	4.324715
F15	Best	**0.000307**	**0.000307**	0.000308	0.000314	0.000312
	Worst	0.020363	**0.001223**	0.120459	0.088541	0.00143
	Mean	0.001485	**0.000399**	0.007588	0.010089	0.001171
	Std	0.004459	**0.000282**	0.026933	0.020407	0.000273
F16	Best	**−1.03163**	**−1.03163**	**−1.03163**	**−1.03163**	**−1.03163**
	Worst	**−1.03163**	**−1.03163**	−0.99999	−0.99999	−1.00018
	Mean	**−1.03163**	**−1.03163**	−1.03002	−1.0253	−1.03005
	Std	**1.25E−16**	1.76E−16	0.007069	0.012979	0.007032
F17	Best	**0.397887**	**0.397887**	**0.397887**	**0.397887**	0.397889
	Worst	**0.397887**	**0.397887**	0.39789	0.397983	0.398107
	Mean	**0.397887**	**0.397887**	0.397888	0.397908	0.397927
	Std	**0.00E+00**	**0.00E+00**	5.33E−07	2.77E−05	5.14E−05
F18	Best	**3**	**3**	**3**	**3**	**3**
	Worst	**3**	**3**	3.000023	30.00016	3.000026
	Mean	**3**	**3**	3.000004	8.400019	3.000003
	Std	6.28E−16	**4.78E−16**	5.43E−06	11.0806	5.99E−06
F19	Best	**−3.86278**	**−3.86278**	**−3.86278**	**−3.86278**	−3.86262
	Worst	**−3.86278**	**−3.86278**	−3.8549	−3.86269	−3.85477
	Mean	**−3.86278**	**−3.86278**	−3.86173	−3.86275	−3.85527
	Std	**2.28E−15**	**2.28E−15**	0.002504	2.27E−05	0.001731
F20	Best	**−3.322**	**−3.322**	−3.32199	−3.3214	−3.13591
	Worst	**−3.2031**	**−3.2031**	−3.13491	−2.43163	−2.06108
	Mean	−3.26255	**−3.26849**	−3.24315	−3.19273	−3.00309
	Std	0.060991	**0.060685**	0.077104	0.197413	0.227568
F21	Best	**−10.1532**	**−10.1532**	**−10.1532**	−10.1119	−10.1351
	Worst	−2.68286	−2.63047	**−5.05519**	−2.61588	−0.35065
	Mean	−8.89864	−9.14865	**−9.64539**	−7.14247	−4.32683
	Std	2.632293	2.494251	**1.562102**	3.341539	4.57182
F22	Best	**−10.4029**	**−10.4029**	**−10.4029**	−10.3678	−10.4004
	Worst	**−10.4029**	−2.7659	−10.4023	−2.70045	−0.90807
	Mean	**−10.4029**	−9.42345	−10.4026	−8.34157	−7.69481
	Std	**2.61E−15**	2.423101	0.000173	3.074106	3.963887
F23	Best	**−10.5364**	**−10.5364**	−10.5363	−10.4781	−10.5232
	Worst	−2.87114	−2.87114	**−10.5358**	−2.41561	−0.94448
	Mean	−9.8181	−9.38662	**−10.5361**	−8.56594	−7.46184
	Std	2.216446	2.808152	**0.000159**	3.314441	3.716296

The best values obtained are in bold.

Table 5
The algorithm parameters and operative restrictions.

Parameters	Value
Number of population	30
Maximum iteration numbers	100
Stallions percentage	0.2
Crossover percentage	0.13
Base MVA	100 MVA
Base kV	12.66 kV
Node system voltage constraints	0.9 pu $\leq V_i \leq$ 1.1 pu
DG's power generation constraints	0 MW $\leq P_{DG} \leq$ 3 MW

Core(TM) i7-8550U CPU @ 1.80 GHz 1.99 GHz, 16 GB RAM, 64-bit operation system (see Table 5).

Figs. 14 and 15 clarify a single-line schematic of these systems (Pothapragada et al., 2020). Real and reactive power consumption for the 33-bus test system is 3715 kW and 2300 KVAR, respectively. The test system's initial power loss is 210.0794 kW, and its minimum voltage is 0.9042 pu. While 69-bus test system's active and reactive power demands are 3802 kW and 2695 KVAR, respectively. The 69-test system's initial power loss is 238.1455 kW, and its minimum voltage is 0.9046 pu. In addition, the IEEE 119-bus test system (11 kV distribution system) with 118 lines (Ali et al., 2020c) has been chosen to check the scalability of the proposed algorithm.

5.2.1. IEEE 33-bus system

Fig. 16 depicts the voltage profile before and after DG insertion. Bus 18 is the furthest endpoint from the substation; therefore, its voltage is the least in the reference scenario (DG absence), and its value is 0.90421 pu. Without DG, buses 6 to 18 and 26 to 33 have the lowest voltage, whereas introducing DG results in a considerable voltage profile improvement within limitations (approved). Furthermore, the usage of DG yields superior outcomes in terms of power loss alleviation.

Table 6 displays the outcomes of the suggested approach for determining the best size, site, and power factor of DG units in a 33-bus system. According to this table, the proportion of power loss depression in the DS is 70.81 percent. Minimum voltages raised from 0.9042 to 0.967 pu as a result.

It is observed that the innovative algorithm results in the least total power loss when compared to those achieved using EA (Mahmoud et al., 2015), Hybrid approach (Kansal et al., 2016), Hybrid Salp Swarm Algorithm (HSSA) (Abdel-mawgoud et al., 2019), PSO (Ali et al., 2020b), SA (Ali et al., 2020b), Improved Analytical (IA) (Kaur et al., 2014), MINLP (Kaur et al., 2014), Hybrid Loss Sensitivity Index and SA (LSISA) (Ali et al., 2020b), Hybrid Loss Sensitivity Index and PSO (LSIPSO) (Ali et al., 2020b), Hybrid SA and PSO (SAPSO) (Ali et al., 2020b), Rider Optimization Algorithm (ROA) (Khasanov et al., 2021), Harris Hawks Optimizer (HHO) (Khasanov et al., 2020), Henry gas solubility optimization (HGSO) (Khasanov et al., 2020), whale optimization algorithms (WOA) (Veera Reddy, 2018), Genetic algorithm (GA) (Hassan et al., 2017), Gray wolf optimizer (GWO) (Kamel et al., 2019), Simplified Analytical Approach (SAA) (Sa'ed et al., 2019), Backtracking search optimization algorithm (BSOA) (El-Fergany, 2015), ALOA (Ali et al., 2016) and Artificial ecosystem-based optimization (AEO) (Khasanov et al., 2020). Fig. 17 depicts the convergence curves of the two techniques (i.e., WHO and IWHO). The findings demonstrate that the IWHO method smoothly accelerates to a correct decision and has stable faster convergence when compared to the WHO algorithm. The IWHO algorithm's invention and notability have been proved and confirmed by identifying the best choice to attain global minima in a short period.

5.2.2. IEEE 69-bus system

While bus 27 is the furthest end of the 69-bus system from the supply node, bus 65 have the lowest voltage value 0.9046 pu because bus 61, which is linked to it, is a strongly loaded point. So, it was chosen as the location for the DG unit. Fig. 18 displayed a significant improvement in the voltage profile.

Table 7 shows the outcomes of the suggested approach for determining the best size, site, and power factor of DG units in a 69-bus system. According to this table, the proportion of power loss depression in the DS is 90.26 percent. Minimum voltages raised from 0.9046 to 0.9725 pu as a result.

According to Table 7, the suggested algorithm has the lowest power loss when compared to the Bat Algorithm (BA) (Khasanov et al., 2019), EA (Mahmoud et al., 2015), Hybrid approach (Kansal et al., 2016), HSSA (Li et al., 2018), PSO (Ali et al., 2020b), Modified PSO algorithm (Ali et al., 2020a), SA (Ali et al., 2020b), IA (Kaur et al., 2014), Mixed Integer Non-Linear Programming (MINLP) (Kaur et al., 2014), Hybrid SA and MPSO (SAMPSO) (Ali et al., 2020a), Rider Optimization Algorithm (ROA) (Khasanov et al., 2021), HHO (Khasanov et al., 2020), HGSO (Khasanov et al., 2020), WOA (Veera Reddy, 2018), GA (Veera Reddy, 2018), SAA (Sa'ed et al., 2019), ALOA (Ali et al., 2016), Cuckoo Search algorithm (CSA), Standard GA (Tan et al., 2012) and Multi-objective

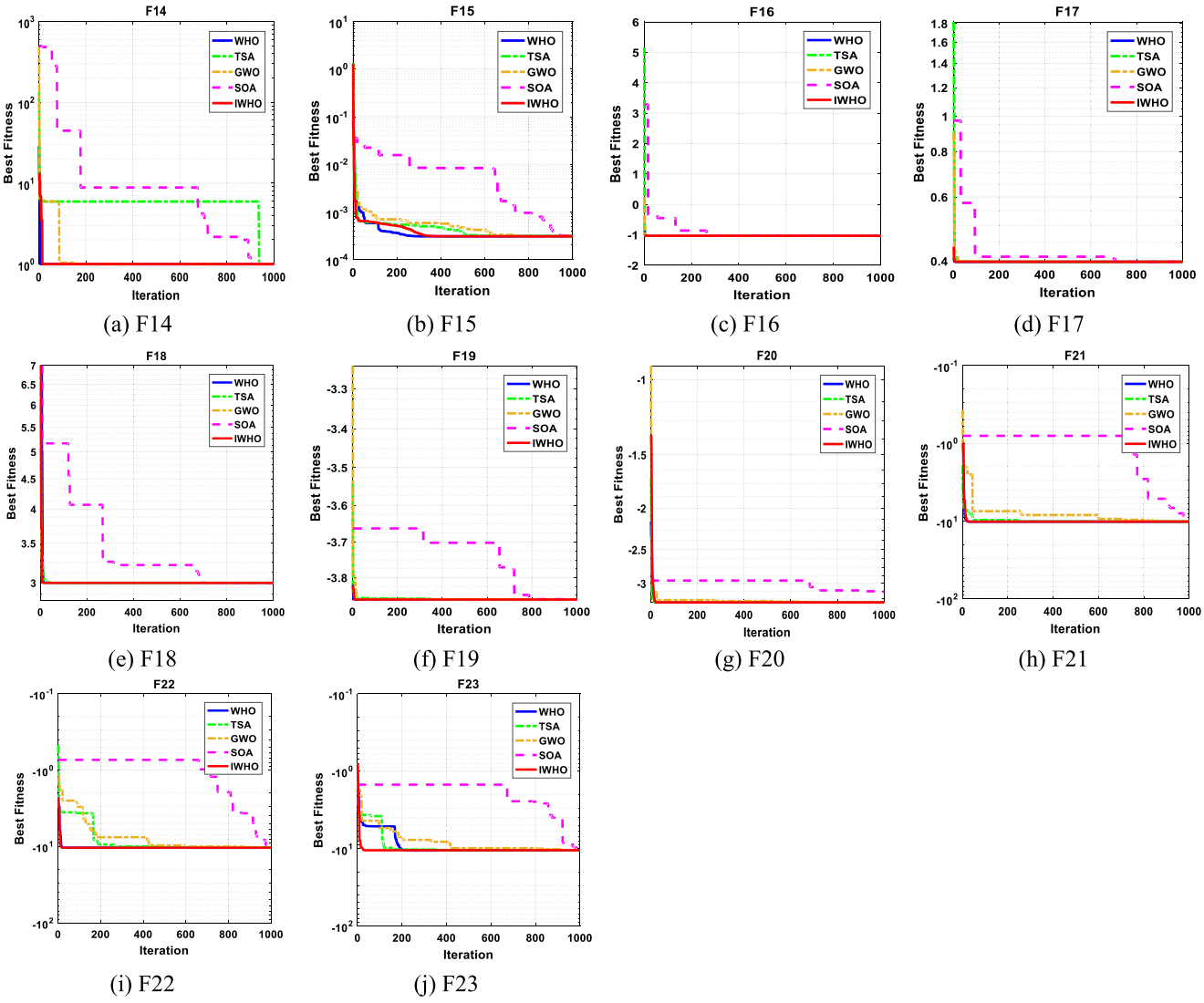

Fig. 12. The convergence curves of all algorithms for composite benchmark functions.

Table 6
The performance analysis of different algorithms in the IEEE-33 bus test system.

Methods	Power losses (kW)	Loss reduction	Min voltage (pu) & Bus number		DG location	DG size P (KW) & Q (KVAR)		Itr
Base case	210.0794	–	0.90421	18	–	–	–	–
SA	70.1894	66.6%	0.95904	18	6	2935.6	1554.8	58
PSO	67.8228	67.7%	0.95862	18	6	2528.3	1747.9	50
LSI-SA	67.8118	67.7%	0.96041	18	6	2556.7	1750.0	28
LSI-PSO	67.8113	67.7%	0.96010	18	6	2658.8	1619.6	33
SA-PSO1	67.8123	67.7%	0.95872	18	6	2557.7	1748.4	10
SA-PSO2	67.8113	67.7%	0.95896	18	6	2511.9	1530.5	18
GA	72.68	64.32%	–	–	6	2831	930.5	–
SAA	67.75	67.89%	–	–	6	2540.84	1737.19	–
GWO	67.87	67.86%	–	–	6	2571.3	1794.77	20
BSOA	82.78	60.76%	0.9549	18	8	1857.4968	1296.54	–
ALOA	71.75	65.99%	0.9528	18	6	1947.756	1103.84	–
HHO	69.443	66.9%	0.95579	18	26	2510.01	1555.56	28
HGSO	68.1743	67.5%	0.9586	18	6	2653.27	1644.345	–
AEO	68.1698	67.55%	0.95830	18	6	2637.42	1634.526	–
HSSA	67.86	67.69%	–	–	6	2547.06	1777.858	–
WOA	78.4337	62.65%	–	–	30	1746.297	845.77	–
EA	67.937	67.66%	–	–	6	2528	1764.55	–
Hybrid	67.9	67.82%	0.9569	18	6	2482.96	1733.11	–
ROA	67.83	67.83%	0.95	18	6	2588.4	1785.77	17
IA	68.157	67.82%	–	–	6	2547.74	1778.33	–
MINLP	67.854	67.7%	–	–	6	2558	1765.55	–
WHO	61.3147	70.81%	0.967	18	6	2541.4727	1742.9416	15
IWHO	**61.3147**	**70.81%**	**0.967**	**18**	**6**	**2541.4727**	**1742.9415**	**6**

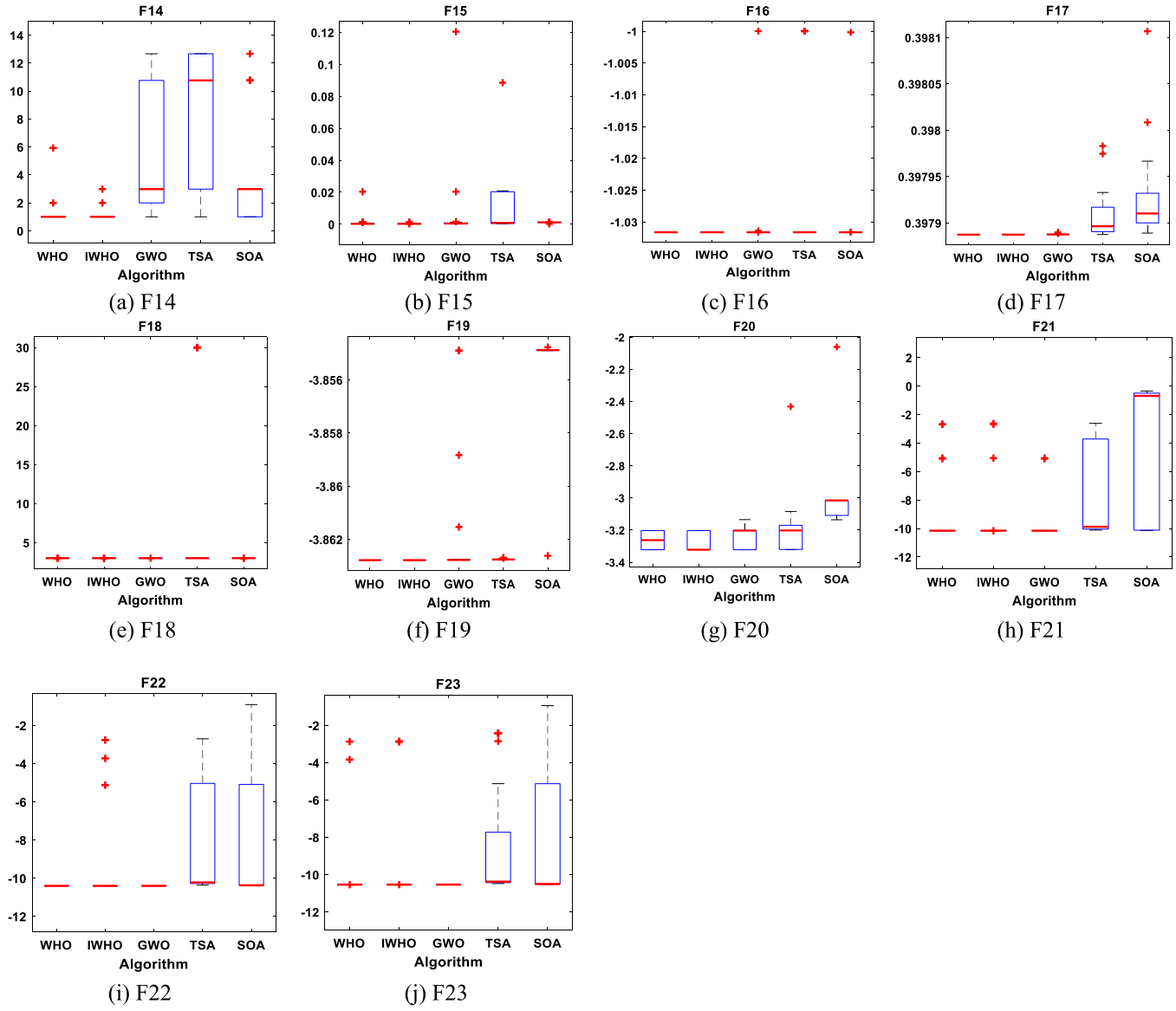

Fig. 13. Boxplots for all algorithms for composite benchmark functions.

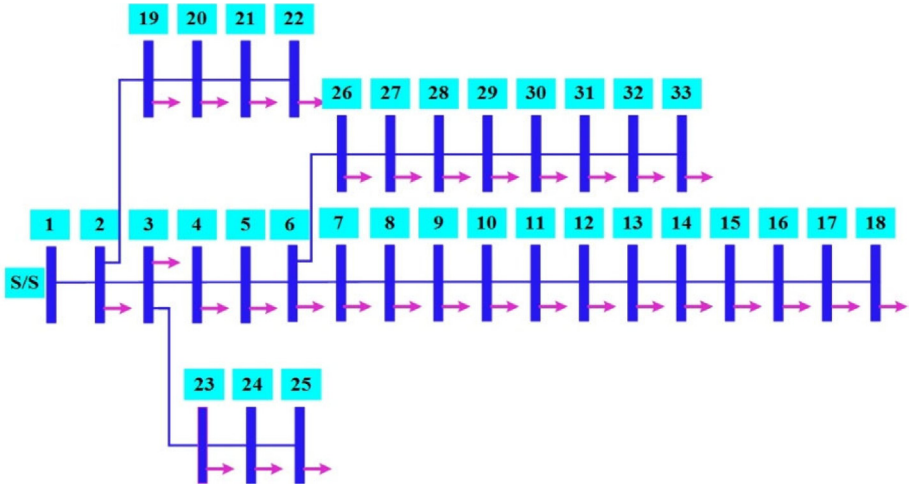

Fig. 14. Standard IEEE-33 bus test system.

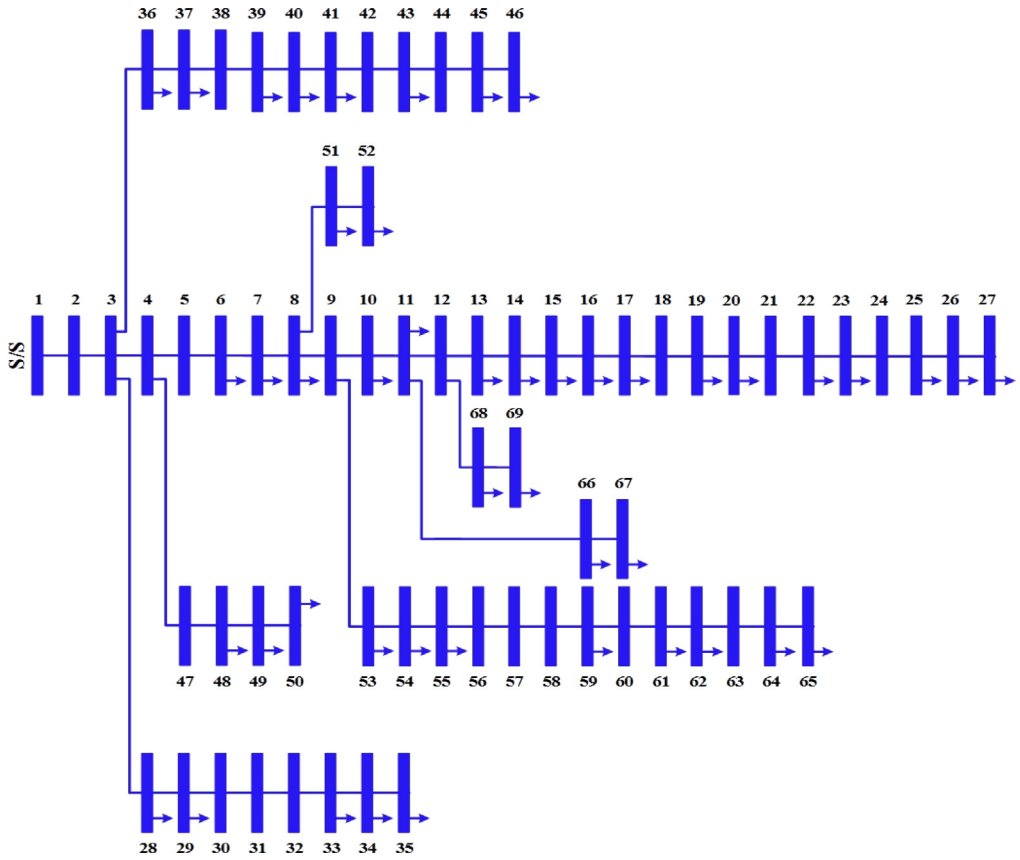

Fig. 15. Standard IEEE-69 bus test system.

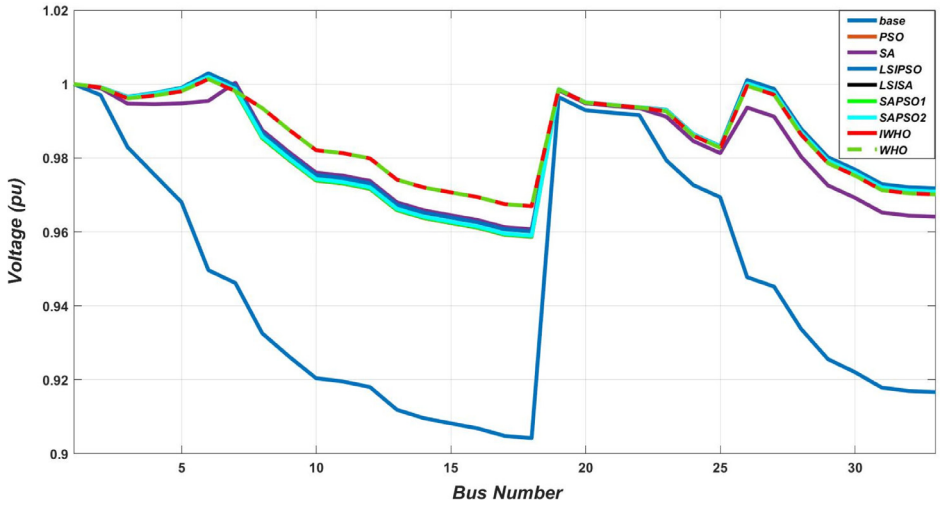

Fig. 16. Voltage profile for IEEE-33 bus test system.

differential evolution (MODE) (Behera and Panigrahi, 2019). Fig. 19 depicts the convergence curves of the two techniques (i.e., WHO and IWHO). The findings demonstrate that the IWHO method smoothly accelerates to a correct selection and has stable faster convergence when compared to the WHO algorithm. The IWHO algorithm's invention and notability have been proved and confirmed by identifying the best option to attain global minima in a short period after 3 iterations.

5.2.3. IEEE 119-bus system

Fig. 20a portrays the voltage profile before and after insertion of one DG unit. It fails to maintain the system voltage within the minimum permissible limits; therefore, two units of DG is used to maintain the system voltage, as illustrated in Fig. 20b, and its minimum value is 0.924 pu at bus 119. Without DG, buses 68 to 78 and 101 to 114 have the lowest voltage, whereas introducing DG results in a considerable voltage profile improvement within limitations (approved). Furthermore, the usage of DG yields superior outcomes in terms of power loss alleviation (see Table 8)

Table 9 shows the outcomes of the suggested approach for determining the best size, site, and power factor of DG units in a 119-bus system. According to this Table, the modified algorithm has the lowest power loss and enhancement voltage profile when

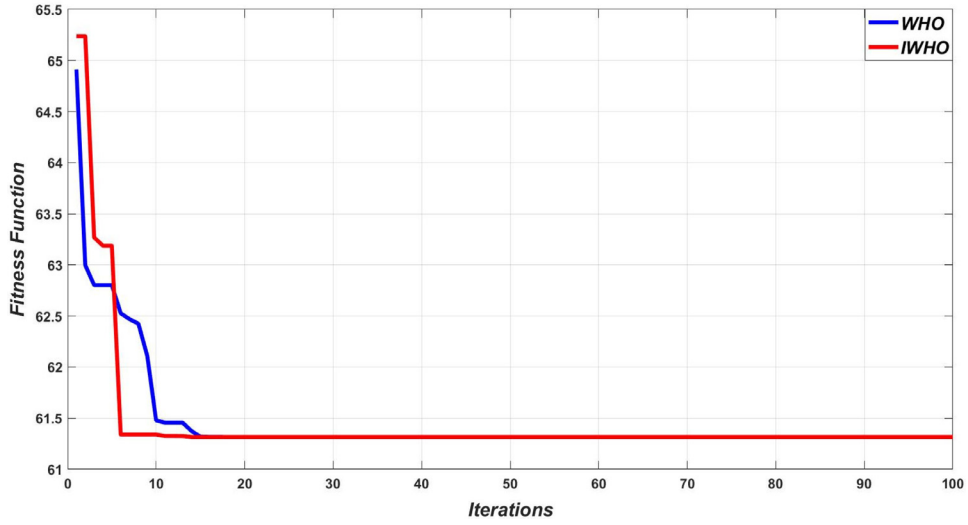

Fig. 17. Convergence curve of the IEEE 33-bus system.

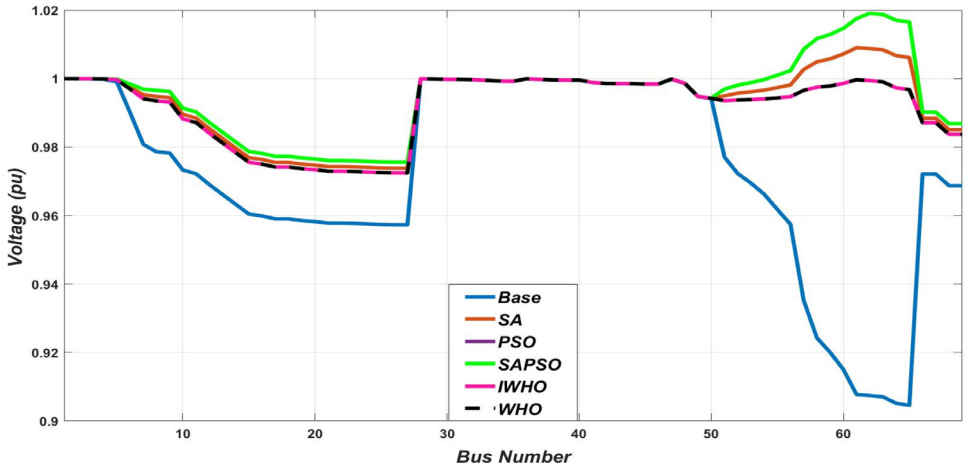

Fig. 18. Voltage profile for IEEE-69 bus test system.

Table 7
The performance analysis of different algorithms in the IEEE-69 bus test system.

Methods	Power losses (kW)	Loss reduction	Min voltage (pu) & Bus number		DG location	DG size P (KW) & Q (KVAR)		Itr
Base case	238.1455	–	0.9046	65	–	–	–	–
SA	26.2583	88.97%	0.9727	27	61	1904.7	1571.9	39
MPSO	23.2358	90.24%	0.9724	27	61	1814.1	1293.3	77
SAMPSO	23.2378	90.24%	0.9738	27	61	1807.0	1295.3	3
GA	38.458	82.9	–	–	61	2047.82	673.085	–
CSA	52.6	76.6	–	–	61	2254	457.694	–
SGA	64.4	71.37	–	–	61	2548	517.39	–
SAA	23.18	89.7	–	–	61	1818.357	1311.74	–
HHO	34.65	85%	–	–	61	1879.41	1311.83	12
HGSO	35.71	85%	–	–	60	1695.9	1360.589	36
BA	52.5	76.67%	–	–	61	2100	426.42	65
PSO	52.5	76.67%	–	–	61	2100	426.42	75
EA	23.26	90.23%	–	–	61	2290	1598.429	–
IA	23.24	90.24%	–	–	61	1839	1283.629	–
Hybrid	23.19	89.7%	–	–	61	1814.4	1313.6	–
MINLP	23.31	90.21%	–	–	61	1828	1299.698	–
MODE	23.20	89.7%	–	–	61	1814.8	1290.314	–
WOA	27.9649	87.57%	–	–	61	1995.66	966.54	–
ROA	23.17	90.27%	–	–	61	1828.47	1304.78	37
WHO	23.178	90.26%	0.9725	27	61	1814.0767	1293.2988	10
IWHO	**23.178**	**90.26%**	**0.9725**	**27**	**61**	**1814.0767**	**1293.2988**	**3**

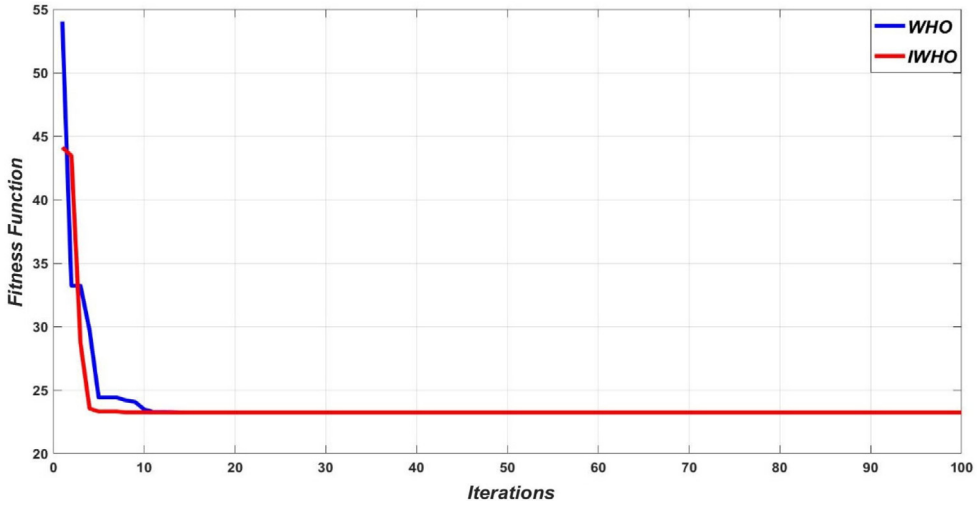

Fig. 19. Convergence curve of the IEEE 69-bus system.

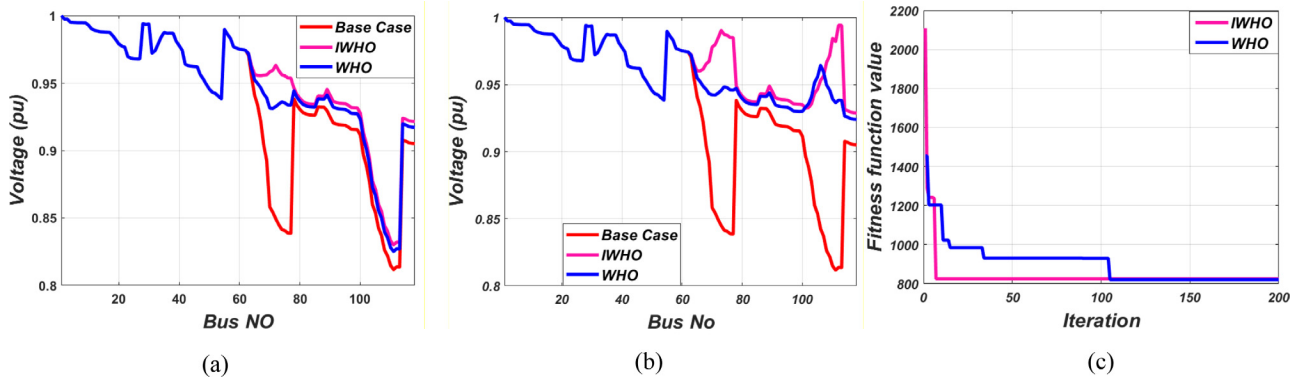

Fig. 20. Voltage profile & convergence curve of the IEEE 119-bus system.

Table 8
The performance analysis of the original and modified algorithms in the IEEE-119 bus test system.

DG type	WHO					IWHO				
	Location	DG size (Kw) (KVAR)		Ploss (kW)	Vmin (pu)	Location	DG size (Kw) (KVAR)		Ploss (kW)	Vmin (pu)
Base case	–	–	–	1235.4	0.81	–	–	–	1235.4	0.81
One DG	74	2281	1783.5	819.5	0.82	72	2484	1814	814.5	0.83
Two DGs	111 66	1333 6117	4518 4128.5	763	0.924	112 67	2243 7550	2871 3933	695.8	0.93

compared to the original algorithm. Fig. 20c illustrates the convergence curves of the two techniques (i.e., WHO and IWHO). The findings demonstrate that the IWHO method smoothly accelerates to a correct selection and has stable faster convergence when compared to the WHO algorithm. The IWHO algorithm's invention and notability have been proved and confirmed by identifying the best option to attain global minima in a short time.

5.3. Reliability analysis

The DG incorporation can improve system reliability as DG can be actively involved in system restoration. The reliability improvement can be maximized if DG units are appropriately allocated with automatic recloser (AR). AR is a safeguard device that can identify a defect and open it for a pre-programmed period before shutting automatically and without the intervention of a human aspect. Figs. 21 and 22 show the modified IEEE 33 & 69 bus test models, including DG and AR. Automatic reclosers/CBs must be used when installing a DG in the DS; otherwise, there'd be no avail because the fault would undoubtedly prevent the DG units from connecting during outages.

A five reliability indicators *CAIDI*, *SAIFI*, *SAIDI*, *ASAI*, and *ENS* are used here to assess the system reliability. Tables 9 and 10 explain the reliability indices for IEEE 33 & 69 bus systems in the base case after applying automatic recloser and applying a dual AR and DG. By comparisons: *SAIFI* is decreased, *SAIDI* is decreased, *CAIDI* is decreased, *ASAI* is increased and *ENS* is decreased, which means that the test systems reliability is improved as indicated in Figs. 23 & 24.

6. Conclusions

An effective optimizer called IWHO has been developed here to mend the performance of the original WHO, which was recently published and applied for the optimal site and size of DGs to slash the operational losses, boost the voltage profile, and

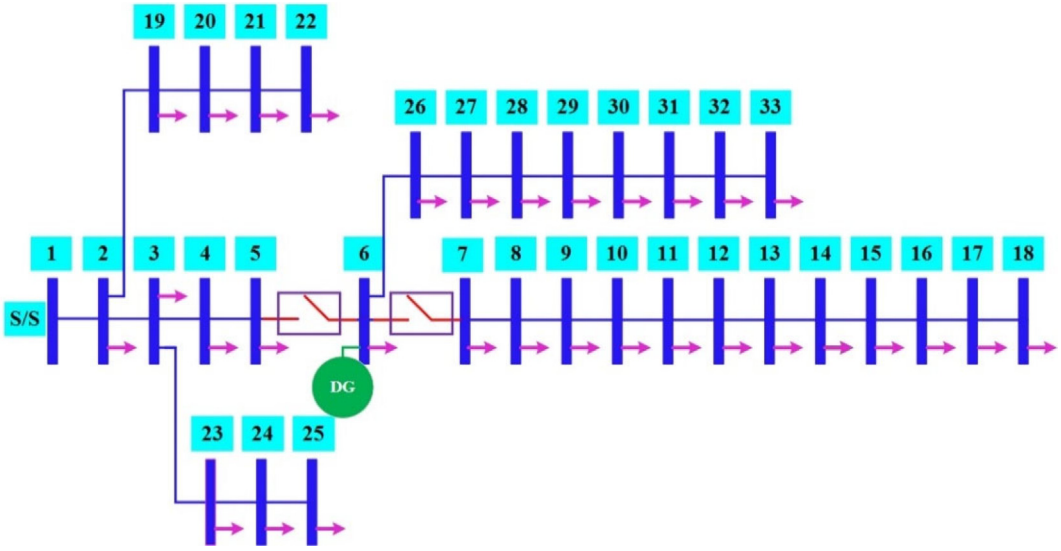

Fig. 21. A modified IEEE 33 bus test.

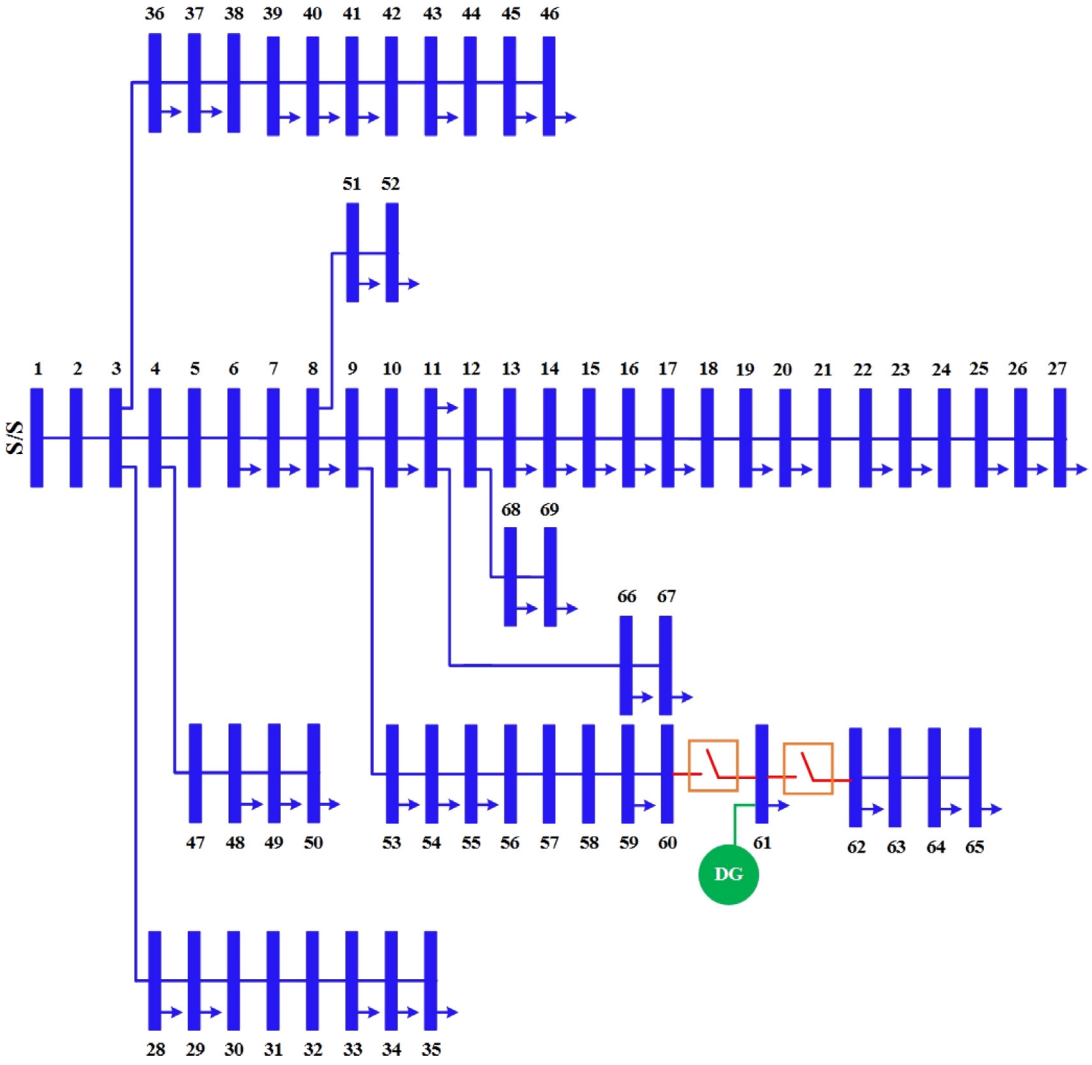

Fig. 22. A modified IEEE 69 bus test.

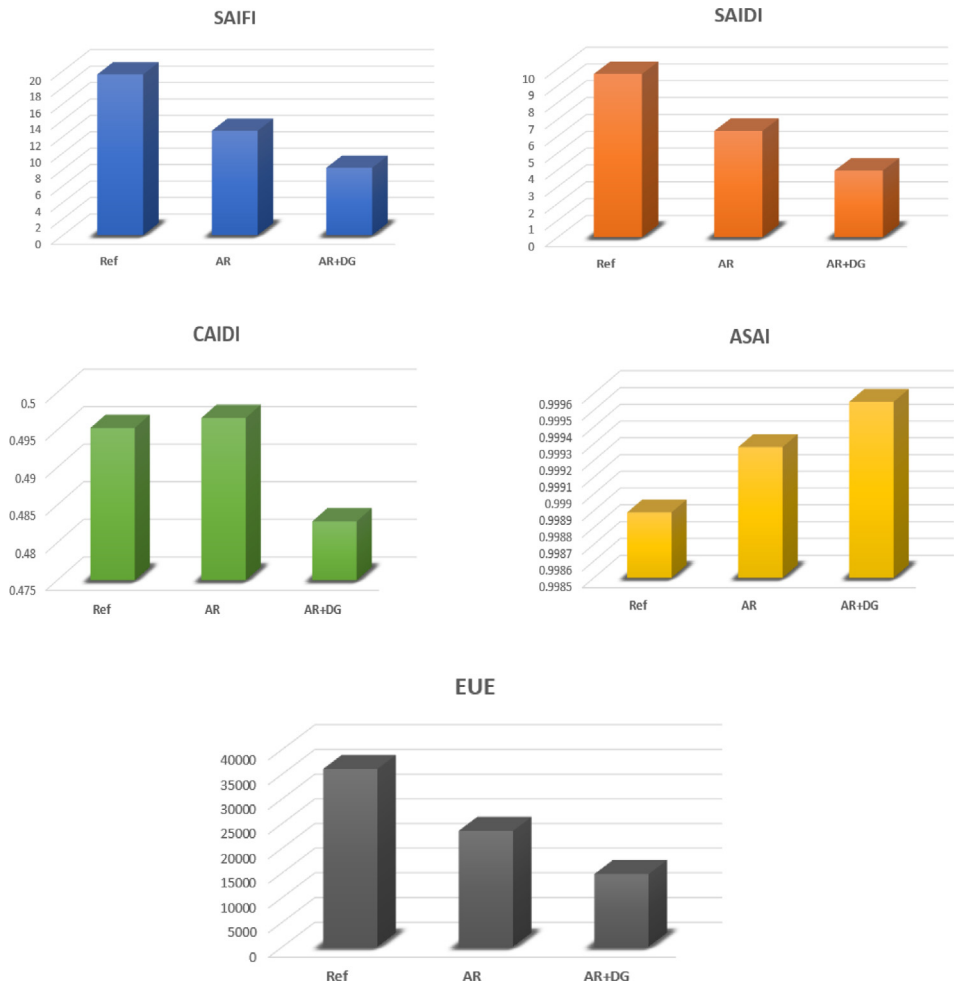

Fig. 23. Comparative results of IEEE-33 system reliability.

Table 9
Reliability indices for IEEE-33 bus system.

Scenario	SAIFI	SAIDI	CAIDI	ASAI	ENS
BASE	19.576	9.6957	0.49529	0.99889	36019.6509
AR	12.7202	6.3171	0.49662	0.99928	23490.4653
AR+DG	**8.2069**	**3.9625**	**0.48283**	**0.99955**	**14 724.8236**

Table 10
Reliability indices for IEEE-69 bus system.

Scenario	SAIFI	SAIDI	CAIDI	ASAI	ENS
BASE	19.609	57.7215	2.9436	0.99341	215 927.917
AR	18.1781	52.7577	2.9083	0.99398	197 296.905
AR+DG	**10.4966**	**30.5274**	**2.9023**	**0.99652**	**116 230.165**

raise the system reliability. The IWHO is created to defeat the weaknesses of the traditional WHO by meliorative the poise between the reconnoitering and utilization and hurry the algorithm convergence. The performance of the developed IWHO algorithm has been verified using 23 benchmark functions, including unimodal, multi-modal, and fixed-dimensional composite functions and it outperformed the four recent algorithms such as Gray Wolf Optimizer (GWO) algorithm, Tunicate Swarm Algorithm (TSA), Sea-gull Optimization Algorithm (SOA), and the original WHO. Also, the effectiveness of the proposed algorithm has been proved using various standards of the IEEE 33-bus and IEEE 69-bus test systems and compared with some meta-heuristic methods to discover its notability. From the findings, it can be seen that the IWHO algorithm lessened the objective function better than other comparative metaheuristic techniques. The simulated results confirm that the IWHO outperforms other compared techniques for solving ODGs problems with optimal power factors in terms of robustness and effectiveness. Lastly, the reliability evaluation is a vital component of distribution system design and planning, and the developed procedure is mainly designed to replicate the random nature of the system and power failure. The acquired findings demonstrate that the technique can guess the probability density function (PDF) of several reliability indices with the necessary precision for systems in the presence and absence of DGs. Because the DG units may actively participate in system recuperation, incorporation of them raises the system reliability. The reliability improvement can be maximized if DG units are appropriately allocated.

The proposed methodology could be used in the integrated planning of smart active distribution networks (ADNs) that face substantial uncertainty from both the generation and load sides in the future study. In addition, our future step work will explore how to handle ADN uncertainties throughout the optimization process by using hybrid energy storage systems, as this allows the produced planning strategies to be more dedicated to actuality.

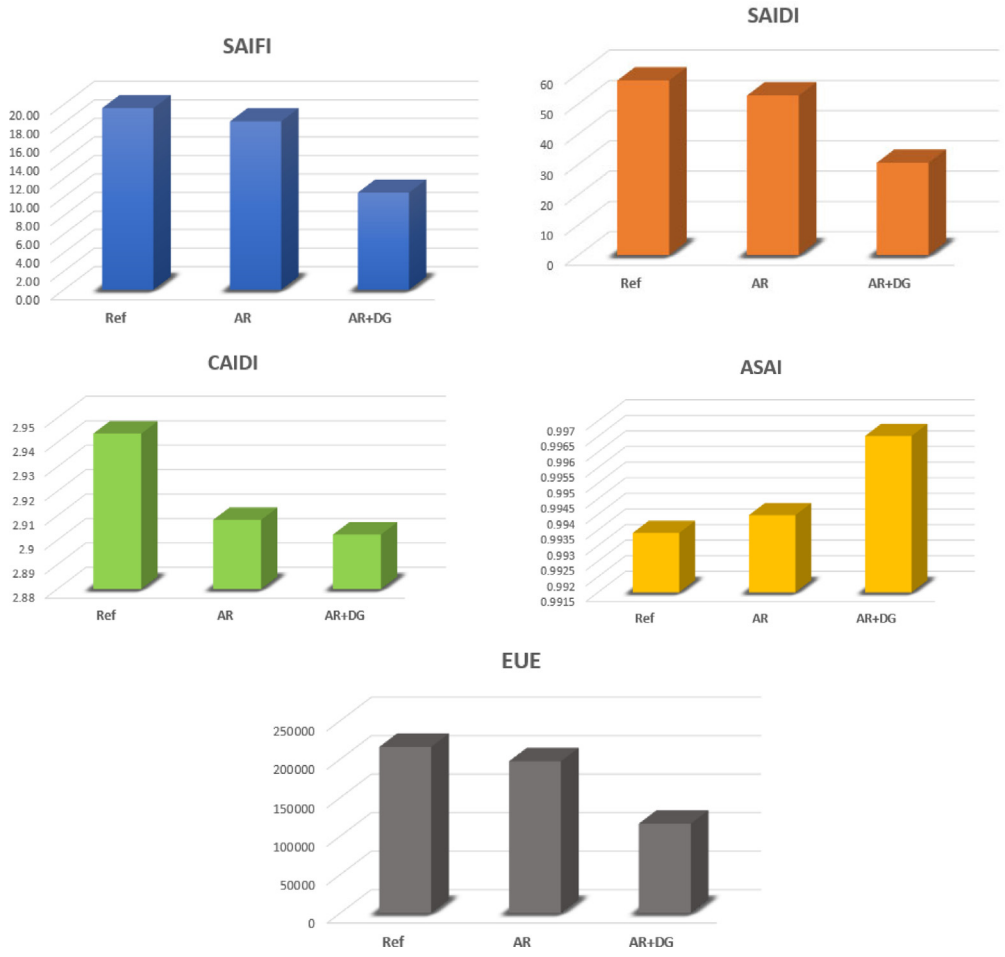

Fig. 24. Comparative results of IEEE-69 system reliability.

CRediT authorship contribution statement

Mohammed Hamouda Ali: Data curation, Methodology, Software, Writing, Reviewing. **Salah Kamel:** Data curation, Methodology, Software, Writing, Reviewing. **Mohamed H. Hassan:** Conceptualization, Validation, Software, Writing, Reviewing. **Marcos Tostado-Véliz:** Supervision, Visualization, Writing – review & editing. **Hossam M. Zawbaa:** Supervision, Writing – review & editing.

Declaration of competing interest

The authors declare that they have no known competing financial interests or personal relationships that could have appeared to influence the work reported in this paper.

Acknowledgments

The author (Hossam M. Zawbaa) thanks the European Union's Horizon 2020 research and Enterprise Ireland for their support under the Marie Skłodowska-Curie grant agreement No. 847402.

References

Abdel-mawgoud, Hussein, Kamel, Salah, Yu, Juan, Jurado, Francisco, 2019. Hybrid salp swarm algorithm for integrating renewable distributed energy resources in distribution systems considering annual load growth. J. King Saud Univ.-Comput. Inf. Sci..

Ali, E.S., Abd Elazim, S.M., Abdelaziz, A.Y., 2016. Ant lion optimization algorithm for renewable distributed generations. Energy 116, 445–458.

Ali, ., Hamouda, Mohammed, Mehanna, Mohammed, Othman, Elsaied, 2020a. Optimal network reconfiguration incorporating with renewable energy sources in radial distribution networks. Int. J. Adv. Sci. Technol. 29 (12s), 3114–3133.

Ali, ., Hamouda, Mohammed, Mehanna, Mohammed, Othman, Elsaied, 2020b. Optimal planning of RDGs in electrical distribution networks using hybrid SAPSO algorithm. Int. J. Electr. Comput. Eng. (IJECE) 10 (6), 6153–6163.

Ali, Aamir, Keerio, M.U., Laghari, J.A., 2020c. Optimal site and size of distributed generation allocation in radial distribution network using multi-objective optimization. J. Mod. Power Syst. Clean Energy 9 (2), 404–415.

Baran, M.E., Hooshyar, H., Shen, Z., Gajda, J., Huq, K.M.M., 2011. Impact of high penetration residential PV systems on distribution systems. In: 2011 IEEE Power and Energy Society General Meeting. IEEE, pp. 1–5.

Behera, Snigdha R., Panigrahi, Bijaya K., 2019. A multi objective approach for placement of multiple DGs in the radial distribution system. Int. J. Mach. Learn. Cybern. 10 (8), 2027–2041.

Billinton, Roy, Wang, Peng, 1999. Teaching distribution system reliability evaluation using Monte Carlo simulation. IEEE Trans. Power Syst. 14 (2), 397–403.

Dehghani, Mohammad, Montazeri, Zeinab, Hubálovský, Štěpán, 2021. Gmbo: Group mean-based optimizer for solving various optimization problems. Mathematics 9 (11), 1190.

Dhiman, Gaurav, Kumar, Vijay, 2019. Seagull optimization algorithm: Theory and its applications for large-scale industrial engineering problems. Knowl.-Based Syst. 165, 169–196.

Dugan, Roger C., Price, Snuller K., 2002. Price issues for distributed generation in the US. In: 2002 IEEE Power Engineering Society Winter Meeting. Conference Proceedings (Cat. No. 02CH37309), Vol. 1. IEEE, pp. 121–126.

El-Fergany, Attia, 2015. Optimal allocation of multi-type distributed generators using backtracking search optimization algorithm. Int. J. Electr. Power Energy Syst. 64, 1197–1205.

Elattar, Ehab E., Elsayed, Salah K., 2020. Optimal location and sizing of distributed generators based on renewable energy sources using modified moth flame optimization technique. IEEE Access 8, 109625-109638.

Eltawil, Mohamed A., Zhao, Zhengming, 2010. Grid-connected photovoltaic power systems: Technical and potential problems—A review. Renew. Sustain. Energy Rev. 14 (1), 112–129.

Essallah, Sirine, Khedher, Adel, Bouallegue, Adel, 2019. Integration of distributed generation in electrical grid: Optimal placement and sizing under different load conditions. Comput. Electr. Eng. 79, 106461.

Gandomi, ., Hossein, Amir, Yang, Xin-She, Alavi, Amir Hossein, 2013. Cuckoo search algorithm: a metaheuristic approach to solve structural optimization problems. Eng. Comput. 29 (1), 17–35.

Hassan, Amal A., Fahmy, Faten H., Nafeh, Abd El-Shafy A., Abu-elmagd, Mohamed A., 2017. Genetic single objective optimisation for sizing and allocation of renewable DG systems. Int. J. Sustain. Energy 36 (6), 545–562.

Hassan, Ahmed S., Othman, ElSaeed A., Bendary, Fahmy M., Ebrahim, Mohamed A., 2020a. Optimal integration of distributed generation resources in active distribution networks for techno-economic benefits. Energy Rep. 6, 3462–3471.

Hassan, ., Shuaibu, Abdurrahman, Sun, Yanxia, Wang, Zenghui, 2020b. Multi-objective for optimal placement and sizing DG units in reducing loss of power and enhancing voltage profile using BPSO-slfa. Energy Rep. 6, 1581–1589.

Huda, ., Nazmul, AS., Živanović, R., 2017. Large-scale integration of distributed generation into distribution networks: Study objectives, review of models and computational tools. Renew. Sustain. Energy Rev. 76, 974–988.

Kadir, Abdul, Fazliana, Aida, Khatib, Tamer, Lii, Loo Soon, Hassan, Elia Erwani, 2019. Optimal placement and sizing of photovoltaic based distributed generation considering costs of operation planning of monocrystalline and thin-film technologies. J. Sol. Energy Eng. 141 (1).

Kamel, Salah, Awad, Ayman, Abdel-Mawgoud, Hussein, Jurado, Francisco, 2019. Optimal DG allocation for enhancing voltage stability and minimizing power loss using hybrid gray wolf optimizer. Turk. J. Electr. Eng. Comput. Sci. 27 (4), 2947–2961.

Kansal, Satish, Kumar, Vishal, Tyagi, Barjeev, 2016. Hybrid approach for optimal placement of multiple DGs of multiple types in distribution networks. Int. J. Electr. Power Energy Syst. 75, 226–235.

Kaur, Sandeep, Kumbhar, Ganesh, Sharma, Jaydev, 2014. A MINLP technique for optimal placement of multiple DG units in distribution systems. Int. J. Electr. Power Energy Syst. 63, 609–617.

Kaur, Satnam, et al., 2020. Tunicate swarm algorithm: A new bio-inspired based metaheuristic paradigm for global optimization. Eng. Appl. Artif. Intell. 90, 103541.

Khasanov, Mansur, Kamel, Salah, Abdel-Mawgoud, Hussein, 2019. Minimizing power loss and improving voltage stability in distribution system through optimal allocation of distributed generation using electrostatic discharge algorithm. In: 2019 21st International Middle East Power Systems Conference (MEPCON). IEEE, pp. 354–359.

Khasanov, Mansur, Kamel, Salah, Rahmann, Claudia, Hasanien, Hany M., Al-Durra, Ahmed, 2021. Optimal distributed generation and battery energy storage units integration in distribution systems considering power generation uncertainty. IET Gener. Transm. Distrib..

Khasanov, Mansur, Kamel, Salah, Tostado-Véliz, Marcos, Jurado, Francisco, 2020. Allocation of photovoltaic and wind turbine based DG units using artificial ecosystem-based optimization. In: 2020 IEEE International Conference on Environment and Electrical Engineering and 2020 IEEE Industrial and Commercial Power Systems Europe (EEEIC/I & CPS Europe). IEEE, pp. 1–5.

Li, Yang, Feng, Bo, Li, Guoqing, Qi, Junjian, Zhao, Dongbo, Mu, Yunfei, 2018. Optimal distributed generation planning in active distribution networks considering integration of energy storage. Appl. Energy 210, 1073–1081.

Liu, Y., Jovan Bebic, B., Kroposki, J., De Bedout, ., Ren, W., 2008. Distribution system voltage performance analysis for high-penetration PV. In: 2008 IEEE Energy 2030 Conference. IEEE, pp. 1–8.

Long, Wen, et al., 2020. A new hybrid algorithm based on grey wolf optimizer and cuckoo search for parameter extraction of solar photovoltaic models. Energy Convers. Manage. 203, 112243.

Mahmoud, Karar, Yorino, Naoto, Ahmed, Abdella, 2015. Optimal distributed generation allocation in distribution systems for loss minimization. IEEE Trans. Power Syst. 31 (2), 960–969.

Mirjalili, Seyedali, Mirjalili, Seyed Mohammad, Lewis, Andrew, 2014. Grey wolf optimizer. Adv. Eng. Softw. 69, 46–61.

Naruei, Iraj, Keynia, Farshid, 2021. Wild horse optimizer: a new meta-heuristic algorithm for solving engineering optimization problems. Eng. Comput. 1–32.

Oree, Vishwamitra, Sayed Hassen, Sayed Z., Fleming, Peter J., 2017. Generation expansion planning optimisation with renewable energy integration: A review. Renew. Sustain. Energy Rev. 69, 790–803.

Pothapragada, Satya Krishna, Mandala, Pruthvi Raj, Hanumandla, Srikanth Reddy, Ravi, Dr. P., 2020. Implementation of expert methodology for optimal reconfiguration in electrical distribution system to minimize I2R losses. Int. J. Adv. Sci. Technol. 29 (3s), 242–254.

Sa'ed, Jaser A., Amer, Mohammad, Bodair, Ahmed, Baransi, Ahmad, Favuzza, Salvatore, Zizzo, Gaetano, 2019. A simplified analytical approach for optimal planning of distributed generation in electrical distribution networks. Appl. Sci. 9 (24), 5446.

Samala, Rajesh Kumar, Kotapuri, Mercy Rosalina, 2020. Optimal allocation of distributed generations using hybrid technique with fuzzy logic controller radial distribution system. SN Appl. Sci. 2 (2), 1–14.

Tan, W.S., Hassan, M.Y., Rahman, H.A., 2012. Allocation and sizing of DG using cuckoo search algorithm. In: 2012 IEEE International Conference on Power and Energy (PECon). IEEE, pp. 133–138.

Transmission, D., Committee, ., et al., 2003. Ieee guide for electric power distribution reliability indices. IEEE Std 1366–2003.

Truong, Khoa H., Nallagownden, Perumal, Elamvazuthi, Irraivan, Vo, Dieu N., 2020. A quasi-oppositional-chaotic symbiotic organisms search algorithm for optimal allocation of DG in radial distribution networks. Appl. Soft Comput. 88, 106067.

Veera Reddy, VC., 2018. Optimal renewable resources placement in distribution networks by combined power loss index and whale optimization algorithms. J. Electr. Syst. Inf. Technol. 5 (2), 175–191.

Walling, R.A., Robert Saint, ., Dugan, Roger C., Jim Burke, ., Kojovic, Ljubomir A., 2008. Summary of distributed resources impact on power delivery systems. IEEE Trans. Power Deliv. 23 (3), 1636–1644.

Zhang, Yanjun, Li, Tie, Na, Guangyu, Li, Guoqing, Li, Yang, 2015. Optimized extreme learning machine for power system transient stability prediction using synchrophasors. Math. Probl. Eng. 2015.